NPS-57Ph75061

NAVAL POSTGRADUATE SCHOOL

Monterey, California

FY75 EXPERIMENTAL HYDRAULIC RAM STUDIES

H. L. Power

June 1975

Final Report for Period 1 July 1974 - 30 June 1975

Approved for public release; distribution unlimited

...red for:
... Weapons Center
... Lake, CA 93555

NAVAL POSTGRADUATE SCHOOL

Monterey, California

Rear Admiral I. W. Linder
Superintendent

Jack R. Borsting
Provost

The work reported herein was supported by the Naval Weapons Center, China Lake, California.

This report was prepared by:

REPORT DOCUMENTATION PAGE

READ INSTRUCTIONS BEFORE COMPLETING FORM

1. REPORT NUMBER: NPS-57Ph75061	2. GOVT ACCESSION NO.
3. RECIPIENT'S CATALOG NUMBER	
4. TITLE (and Subtitle): FY75 Experimental Hydraulic Ram Studies	5. TYPE OF REPORT & PERIOD COVERED: Final Report 1 July 1974 - 30 June 1975
6. PERFORMING ORG. REPORT NUMBER	
7. AUTHOR(s): H. L. POWER	8. CONTRACT OR GRANT NUMBER(s)
9. PERFORMING ORGANIZATION NAME AND ADDRESS: Naval Postgraduate School, Monterey, California 93940	10. PROGRAM ELEMENT, PROJECT, TASK AREA & WORK UNIT NUMBERS: N6053075P000011
11. CONTROLLING OFFICE NAME AND ADDRESS: Naval Weapons Center, China Lake, California 93555	12. REPORT DATE: June 1, 1975
	13. NUMBER OF PAGES
14. MONITORING AGENCY NAME & ADDRESS (if different from Controlling Office)	15. SECURITY CLASS. (of this report): UNCLASSIFIED
	15a. DECLASSIFICATION/DOWNGRADING SCHEDULE

16. DISTRIBUTION STATEMENT (of this Report)

Approved for public release; distribution unlimited.

17. DISTRIBUTION STATEMENT (of the abstract entered in Block 20, if different from Report)

18. SUPPLEMENTARY NOTES

19. KEY WORDS (Continue on reverse side if necessary and identify by block number)

Aircraft Survivability
Aircraft Vulnerability
Fuel Cells
Hydraulic Ram

20. ABSTRACT (Continue on reverse side if necessary and identify by block number)

This document is a report on the progress of FY 75 experimental Hydraulic Ram Studies. The shock and drag phases of hydraulic ram were studied to understand this complicated phenomenum.

Table of Contents

I. Introduction

In recent years the study of failure of aircraft fuel cells caused by encounter with ballistic threats has become increasingly important. Projectiles that penetrate fluid filled cells cause damage many times greater than that incurred by impact with an empty cell. This interaction is called Hydraulic Ram. Hydraulic ram may be studied by identifying several phases which are named after the dominant projectile energy dissipation mechanism. These phases and their effects on fuel cell wall response occur during different time scales. The phases usually identified are:

1. a penetration phase where the projectile punches a hole in the entry wall
2. a shock phase during which projectile protusion into the fluid drives a hemispherical shock wave into the tank liquid
3. a drag phase during which projectile energy is dissipated by form drag and a cylindrical vapor filled cavity is formed
4. a cavity oscillation phase which results from the growth and eventual collapse of the drag phase cavity

This report presents the results of experimental studies designed to substantiate current fuel cell internal and wall pressure prediction models for the shock and drag phases of hydraulic ram, and to measure the entry wall response to these loadings.

II. Shock Phase Pressures

Several investigators[1,2,3] have shown that projectile protusion into a fuel cell produces a hemispherical shock wave which is centered at the impact point. Projectile momentum and path after entry have no observable effect on the shock shape as it propagates into the fluid. Since impacts with obliquity also exhibit this characteristic it was concluded that shock phase characteristics may be modeled as the result of a point energy source release. The theory of Yurkovich[4] is based upon this assumption. The theory assumes a rigid entry wall and shock radius that is proportional to a constant power of time. Spark shadowgraph experiments[1,2,3] have shown that blunt projectiles (spheres, shells with hemispherical noses, and warhead fragments for example) exhibit a shock radius that is proportional to the 0.8 power of time and that projectiles with ogive nose shape produces a shock radius that is proportional to the 0.9 power of time.

The flow field was calculated by coupling the one-dimensional Rankine-Hugoniot equations with the Tait equation of state for isothermal compressible liquids to determine shock front jump conditions as a function of the shock Mach number. Using the normal strong shock assumptions, the radial distribution of the flow parameters behind the front was then determined by assuming a power law density distribution and integrating the continuity equation to determine the radial velocity distribution. The momentum equation was then integrated to determine the pressure distribution. Given a shock phase energy release E_o the shock Mach number as a function of radius was determined from energy considerations.

The theory of Yurkovich gives no information as to the value of the energy release during the shock phase. Figure II-1 shows a qualitative

view of projectile velocity decay during hydraulic ram. It is known that in most instances only a portion of the impact energy E_i transferred during shock formation since projectiles travel many inches into the tank before coming to rest. In the shock formation region projectile velocity drops sharply as a result of shock formation. Velocity decay after shock formation is due to projectile form drag. If the projectile is considered to be a piston in the early stages of shock formation, the rate of change of fluid volume displaced would determine the momentum exchange between the projectile and the fluid, hence the shock strength. It may be assumed that a characteristic time for shock formation would be that required for the projectile to penetrate the fluid an axial distance equal to that at which the projectile maximum cross-sectional area occurs. The shock formation characteristic time is no longer than a few microseconds for most cases of interest. It may also be deduced that the projectile Mach number with respect to the fluid has an important role in determining the strength of the shock and therefore the amount of energy deposited during the shock phase. An analytical expression for the shock phase energy release as a function of projectile, wall, and fluid properties is not available to date. Information about the shock formation process could be calculated numerically using computer codes similar to those used to study projectile penetration dynamics of multiple element targets. Use of this method, however would require a systematic parameter study which would involve large expenditures of computer time. Experimental studies of projectile decelleration during hydraulic ram have been made by Stepka[2] and Kapple[3]. Projectile position as a function of time was measured using shadowgraphs. These measurements of the velocity decay of spheres with various diameters, masses, and impact velocities indicates

that the energy deposited during shock formation is a constant percentage of the impact energy and is primarily a function of the projectile impact Mach number with respect to the fluid. Figure II-2 shows the observed dependance of the change in projectile velocity ΔV_s occuring during the characteristic shock formation time with projectile impact Mach number. Little data was available for times on the order of a few microseconds, hence, the data was extrapolated to small times for these calculations. Impact Mach numbers which are less than sonic produce a shock formation velocity decay which is less than 10 percent of the impact velocity. For impact Mach numbers greater than sonic the loss in projectile velocity raises rapidly to approximately 80 percent at a Mach number of 3.5. Figure II-2 also shows the corresponding shock phase energy input percentage as a function of Mach number. This information was used in conjunction with the theory of Yurkovich to estimate shock phase pressures during hydraulic ram. These data indicate that the shock phase becomes increasingly important as projectile impact Mach number increases since a supersonic projectile will generate stronger shock phase pressures than a subsonic projectile of the same impact energy.

Computer calculations[5] based upon the Yurkovich theory show that the shock is attenuated by spatial and viscous effects very quickly and becomes acoustic. Figure II-3 shows that the distance traveled into the fluid and the time from impact at which the wave speed is sonic for tanks filled with water and with aviation fuel. Figure II-4 shows a typical pressure distribution resulting from the impact of a 45 grain .222 caliber small arms projectile with a water filled tank. The wave produced becomes acoustic at approximately 14 microseconds after impact and at a distance of one inch from the impact point. The pressure distribution for times larger than that required for the wave to reach sonic speed was

calculated using acoustic wave theory. Intense pressures are predicted near the entry point but the pulse is quickly reduced in magnitude to several thousand pounds per square inch at a distance greater than an inch. Figures II-5 through 7 show similar predicted pressure distributions resulting from the impact of a 50 caliber, 12.7 mm and 14.5 mm threat in a fuel filled tank.

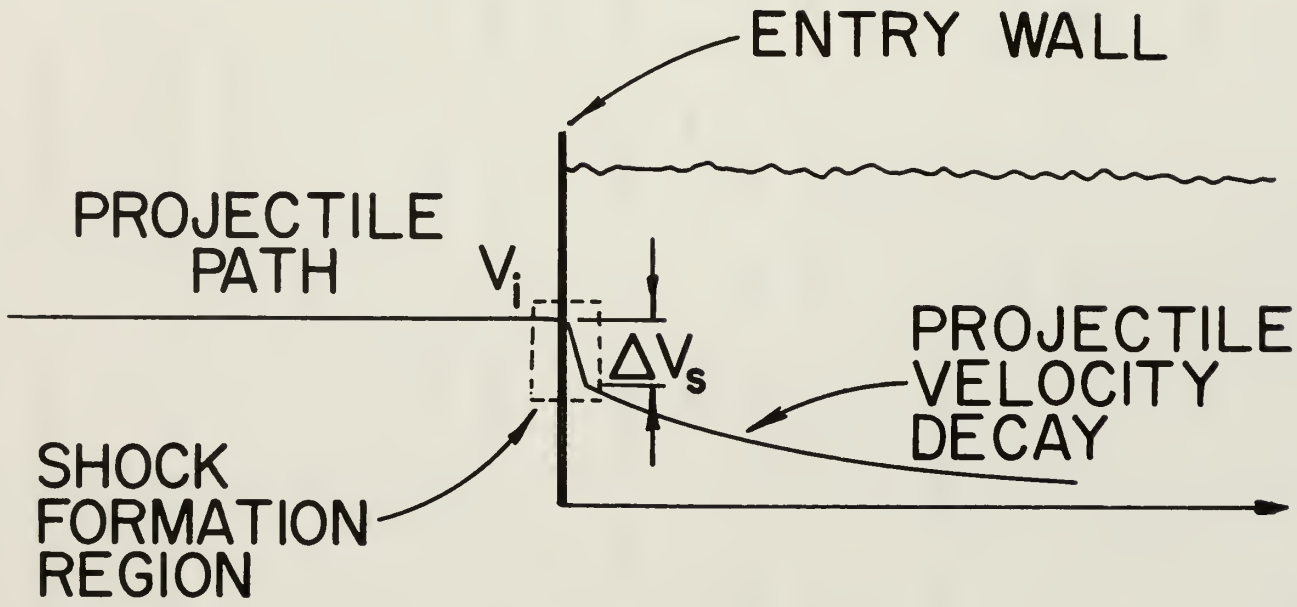

FIG. II-1 QUALITATIVE VIEW OF PROJECTILE VELOCITY DECAY DURING HYDRAULIC RAM

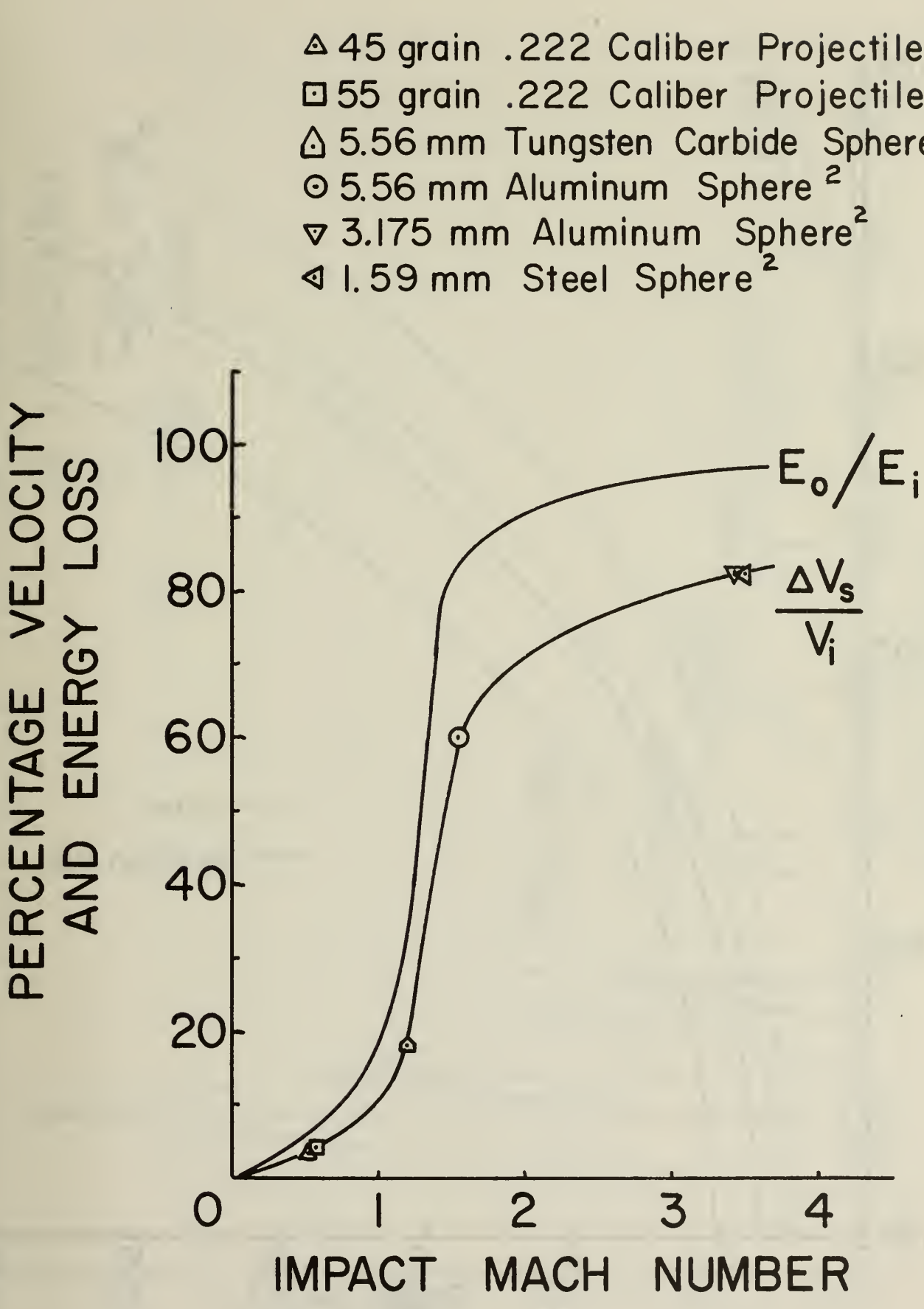

FIG. II-2 SHOCK PHASE ENERGY RELEASE

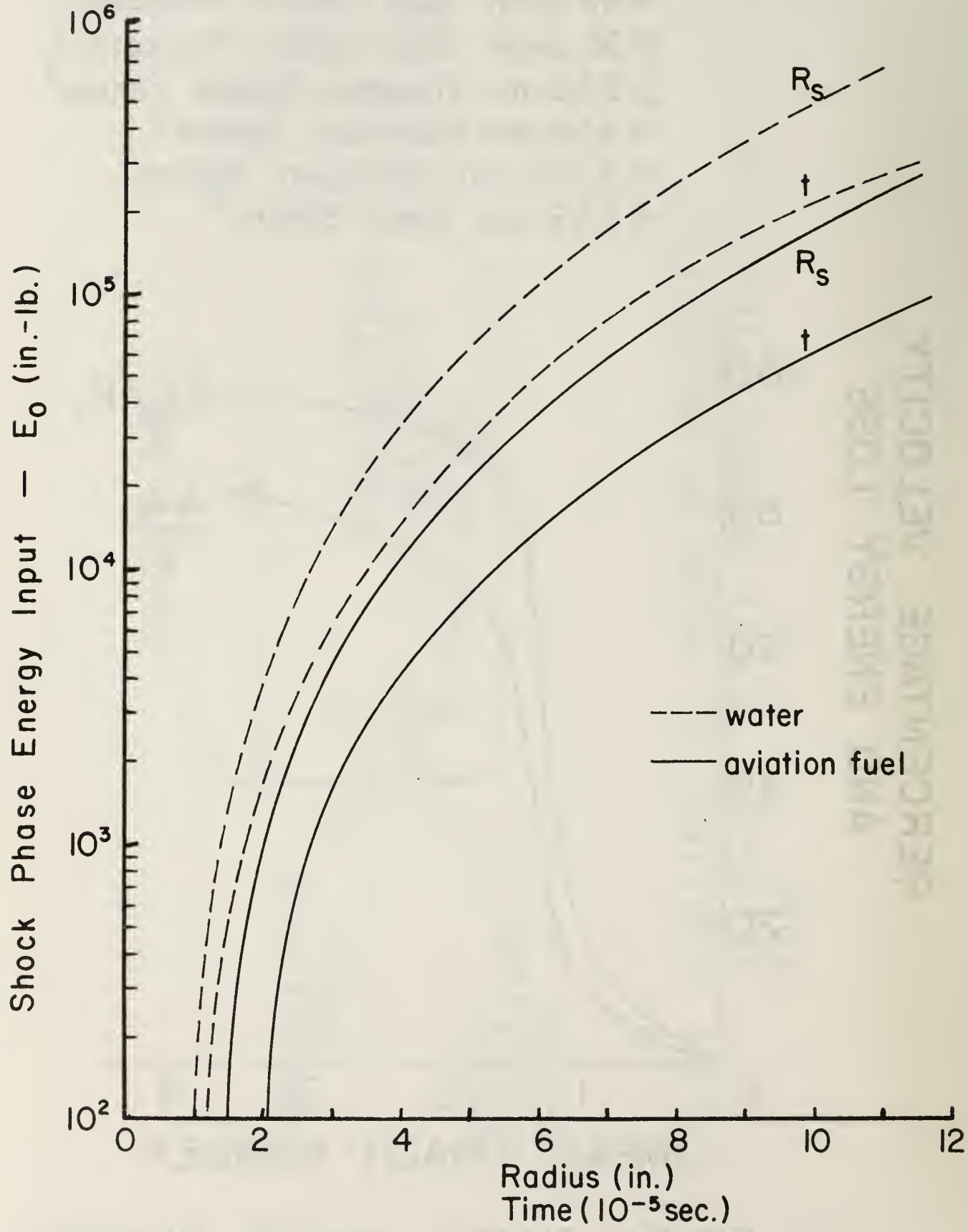

FIGURE II-3 RADIUS AND TIME FOR ACOUSTIC SHOCK SPEED

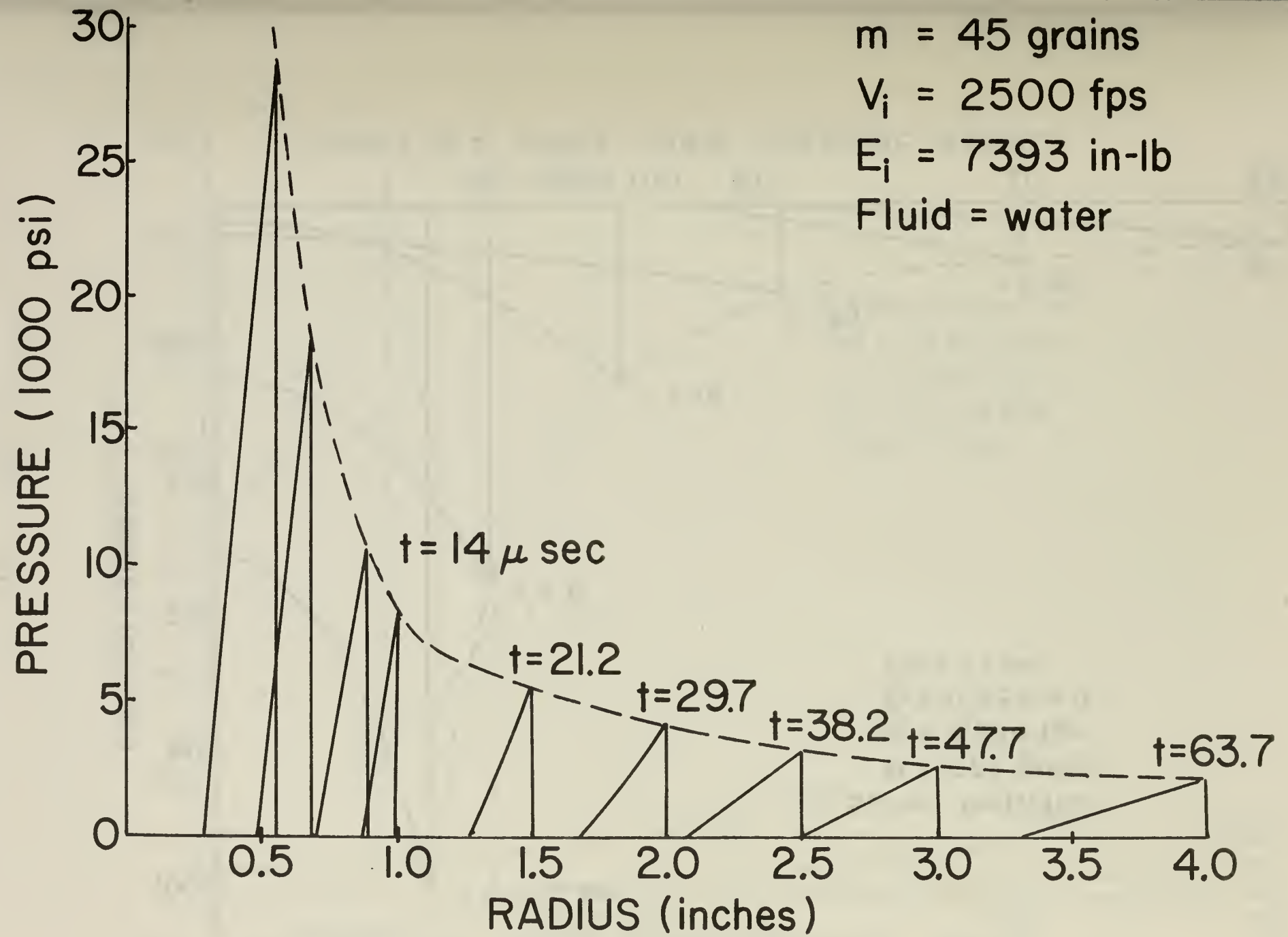

FIG. II-4 SHOCK PHASE PRESSURE FOR .222 CALIBER PROJECTILE

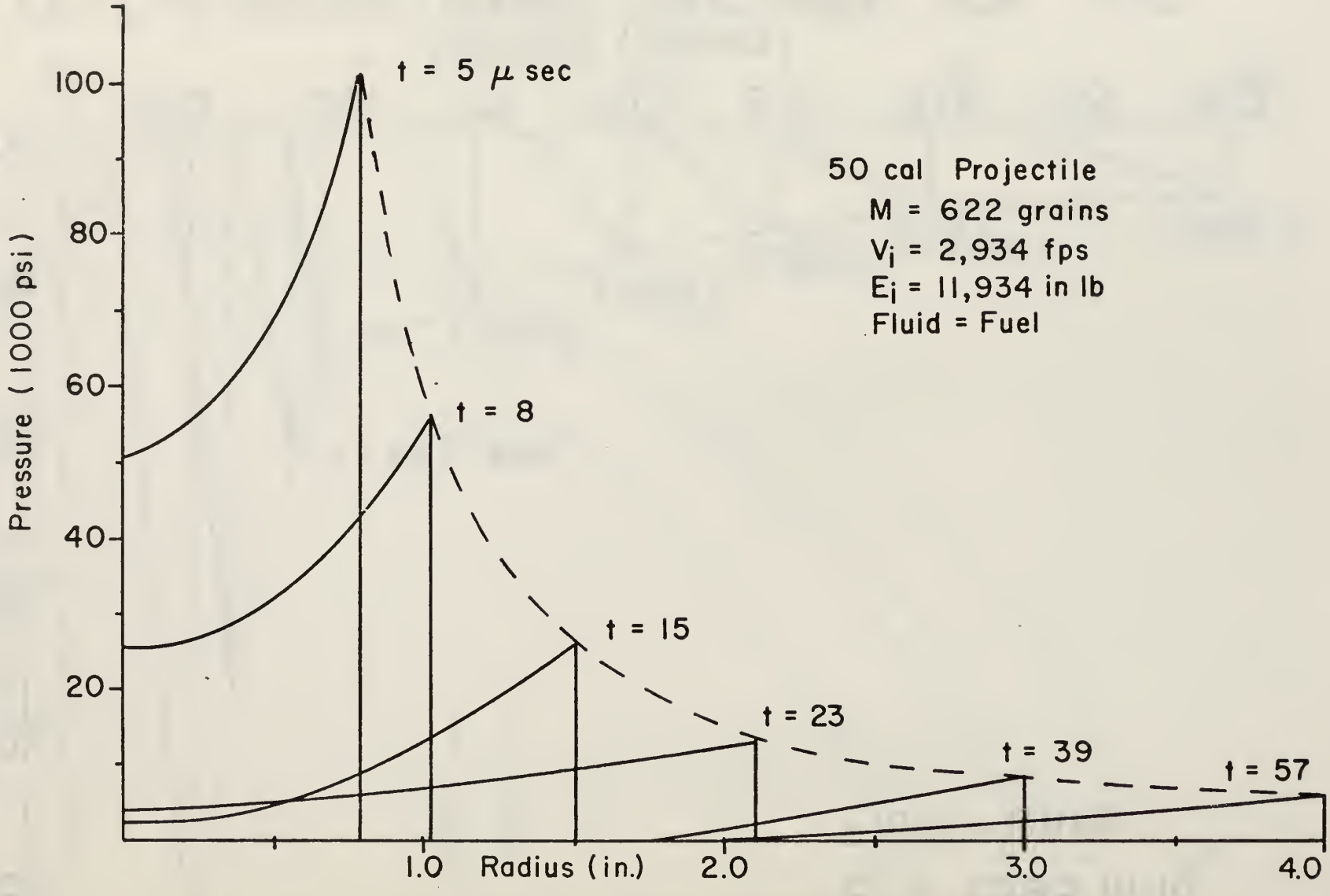

FIGURE II-5 SHOCK PHASE PRESSURE PROFILE

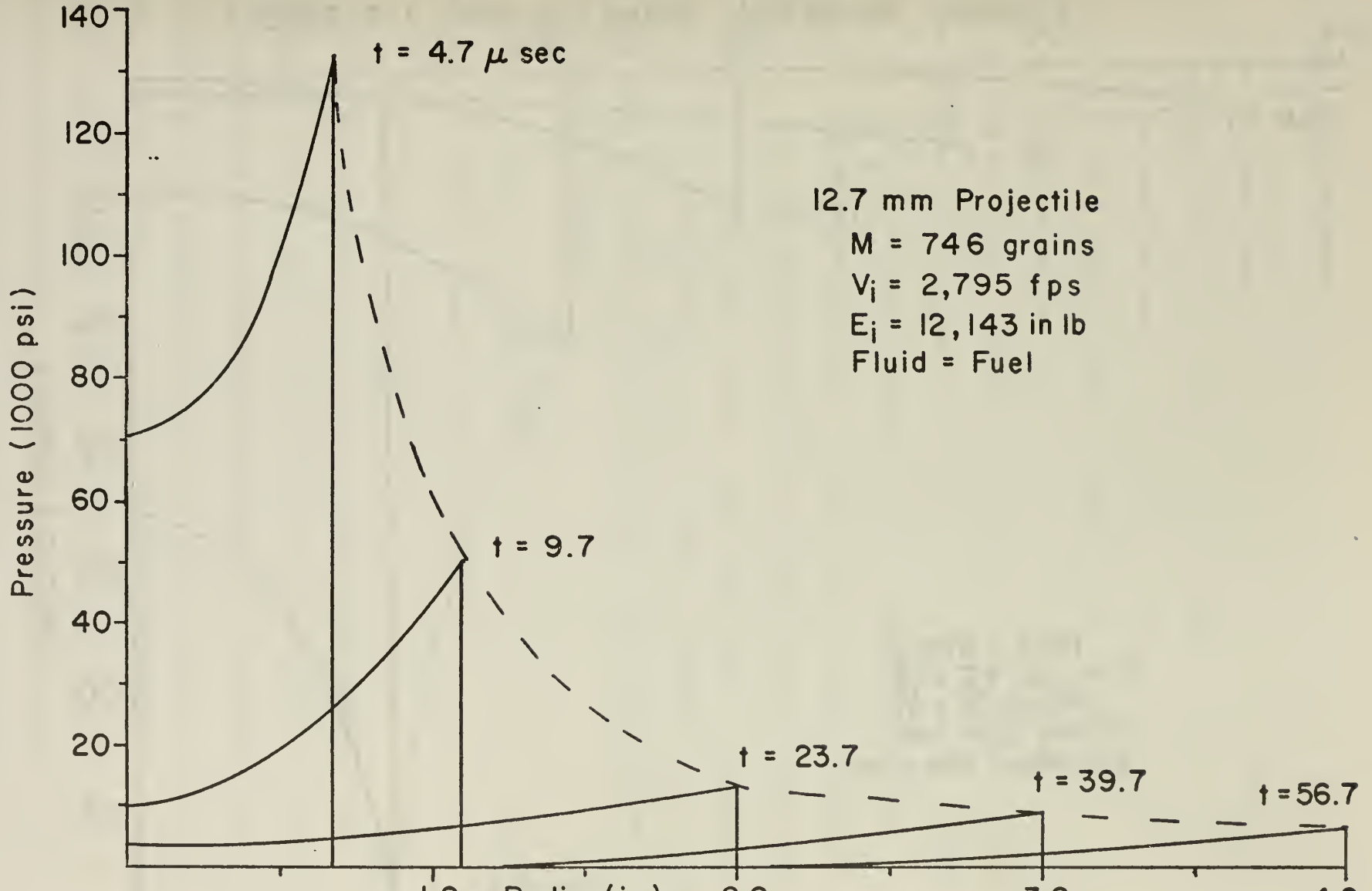

FIGURE II-6 SHOCK PHASE PRESSURE PROFILE

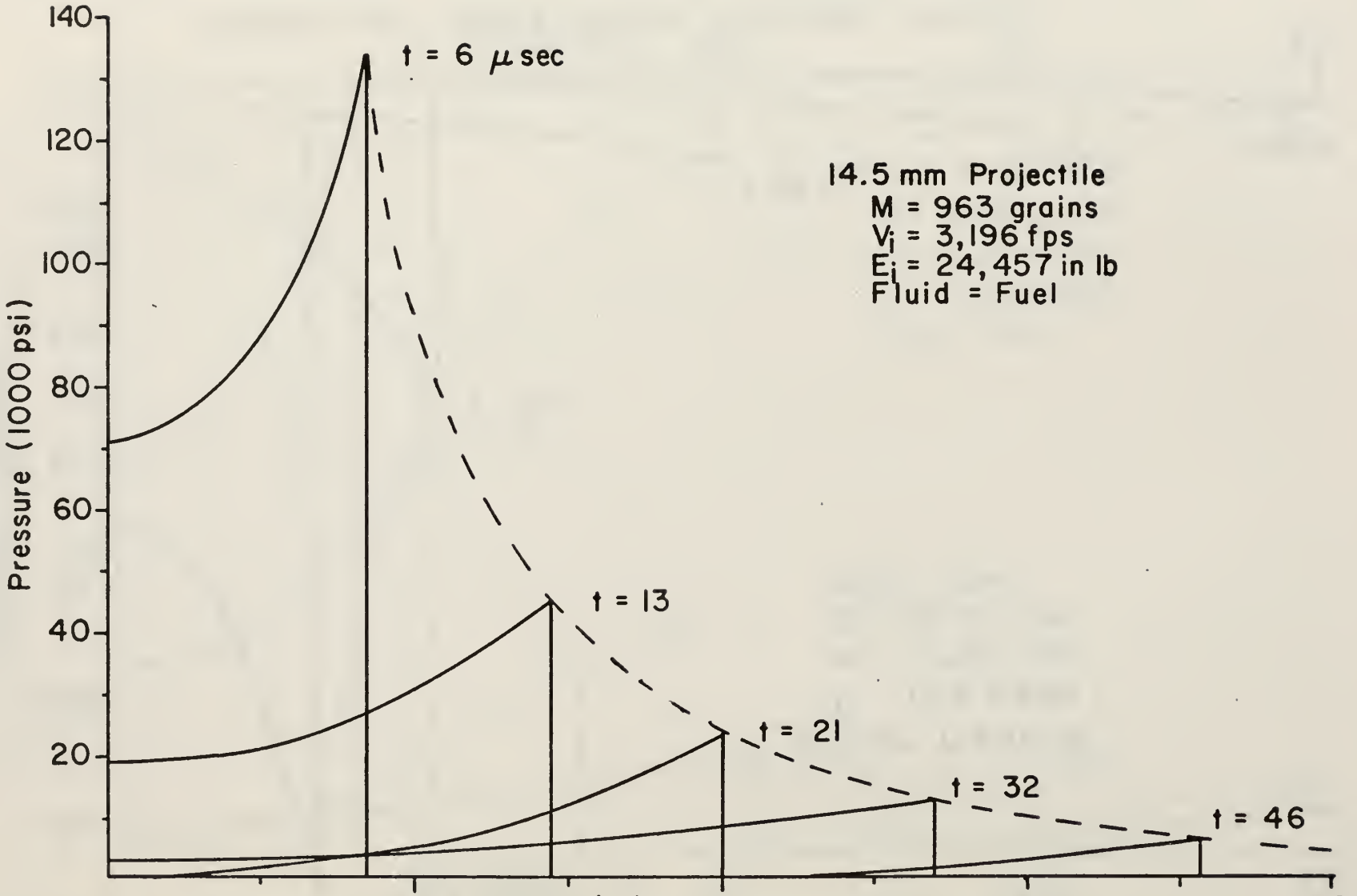

FIGURE II-7 SHOCK PHASE PRESSURE PROFILE

III. Drag Phase Pressures

Since the shock phase, in most cases of interest, does not dissipate all the available energy the projectile travels through the fuel cell fluid until the remaining energy is dissipated or until the exit wall is impacted. During this drag phase of hydraulic ram a cylindrical cavity, whose size is dependant upon the rate of kinetic energy loss along the trajectory, is formed. Projectile spin and angle of attack combine to produce Magnus sideforces which pertrub the projectile from a straight path. Lift production usually causes projectile instability and the projectile tumbles a few inches from the entry point. Large stagnation pressures in the flow can cause projectile deformation and in some cases the projectile does not remain intact. These factors made an analytical estimation of the drag phases pressures difficult. Lundstrom[6] has analyzed the drag phase by assuming a simple drag equation which results in an energy loss rate given by:

$$\frac{dE}{dx} = mBV^2 \qquad \text{(III-1)}$$

where B is the velocity decay coefficient defined as:

$$B = \frac{\rho_f C_d A}{2m} \qquad \text{(III-2)}$$

The wave equation was used to calculate the flow field resulting from projectile and cavity motion. The projectile and cavity were approximated by a distribution of sources along the trajectory. The velocity potential was expressed as an integral function of the source strength distribution, spatial position, and time. The source strength distribution was estimated by equating the drag phase energy deposited by the projectile to the sum of the work done by the difference in ambient and cavity pressure and the kinetic energy contained in the tank fluid. Restraining effects of the

fuel cell walls on cavity growth are neglected and this method cannot predict source strength during cavity collapse. The pressure fluid resulting from the source distribution was calculated from the change in potential with time. Wave reflections from fuel cell walls were calculated using the method of images but waves reflected from the cavity surface are ignored. Fuel cell pressure predictions are very dependant upon the assumed motion of the tank walls. For times less than several hundred microseconds (which is characteristic of the duration of the shock and drag phase) entry wall reflected waves are of primary importance. Lundstrom's analysis can predict fuel cell pressures for two types of wall response: the rigid or stationary wall and the free surface. Thin walled fuel cell internal pressures may be estimated by assuming the walls are free surfaces. Cole[7] has shown that an exponential plane wave impinging upon thin walls that are typical of aircraft fuel cell construction are reflected very nearly as if the wall were a free surface. This assumption, however, eliminates accurate prediction of wall pressure loadings that are necessary to predict wall motion and stress during hydraulic ram.

Accurate prediction of fluid pressures near the walls requires the solution of a coupled fluid-structure interaction problem. Ball's[8,9,10] application of piston theory to this problem, however, allows the structure and fluid equations to be uncoupled. This theory requires only the knowledge of the pressure and velocity that would exist if the wall were not there, including earlier reflections from other walls and free surfaces. This incident pressure and velocity information can be obtained from Lundstrom's analysis and wall strains during hydraulic ram may be estimated.

Experimental Results

A series of experiments[3,11,12] were undertaken using a simple tank configuration to determine hydraulic ram pressure loadings for two .222 caliber threat energy levels. The test fuel cell was cubical with inside dimensions equal to seventeen inches, and was constructed by welding one quarter inch by three inch aluminum angle sections to form a frame. Side and bottom walls were one inch thick plexiglass and the entry and exit walls were bolted to the frame so that various thicknesses and materials could be tested. The top was open and bullet entry into the tank with minimum loss of energy was accomplished by providing a one inch dimater hole in the center of the entry wall. A .222 caliber rifle was used to fire copper-jacketed lead projectiles whose mass and impact velocity was adjusted to obtain the 7,493 in-lb and 12,323 in-lb impact energy levels tested. Spark shadowgraphs were taken during hydraulic ram to determine shock phase wave shape, shock position and projectile location as a function of time. Shock phase wave shape was found to be hemispherical and the shock radius was proportional to the 0.9 power of time for the projectiles studied. Projectile position data was used to evaluate the projectile velocity decay coefficient B used in the Lundstrom drag phase analysis. These data were used to predict shock and drag phase internal tank pressures. Kistler 603H quartz pressure transducers were mounted in the tank to measure internal pressure at a given spatial position verses time. Pressures were measured along a line inclined 50° from the vertical at radii varying from two to eight inches from the impact point.

Holm[11] measured the internal pressures resulting when a 0.5 inch thick steel plate was used as the entry wall. This stimulates the case of a rigid entry wall. Figures III-1 through 3 show a comparison of the

estimated and measured pressure for the low energy level threat and Figure III-4 through 6 show the higher energy level threat. The calculations predict two pressure pulses of very different time scales. The shock phase pulse is large in magnitude but very short in duration (less than 25 microseconds). The drag phase pulse, however, has approximately one-half peak shock phase magnitude and a duration of approximately one hundred microseconds. The experimental data does not exhibit the characteristics of the predicted shock phase pressures. The transducer used has a rise time of one microsecond but the charge amplifier used to condition the transducer output has a frequency response of 300 KH_z. It was expected, therefore, that the shock phase pulse would not be accurately reproduced at the output. Yeteerbium piezoresistive transducers with response characteristics suitable for measurement of shock phase pulses have been developed at the Stanford Research Institute[13] but these thin film gages are destroyed in a few microseconds after shock front passage. Until better pressure transducers systems with rise times of approximately 10 nanoseconds are developed and become commercially available the validity of shock phase pressure predictions cannot be established. The calculation of shock phase pressure assumes a rigid entry wall. Wall motion in response to the shock phase loading may produce rarefraction waves which significantly distort the predicted distribution of pressure near the wall.

The experiments do exhibit characteristics similar to the predicted drag phase pulse. The time scale and peak pressure magnitude of this pulse is accurately predicted but the pulse shape is not. The drag phase peak magnitude comparison is shown in Figure III-7. The pulse shape discrepancy was due to the assumption of a constant drag coefficient along the trajectory. The shadowgraph records of projectile position could not be used to determine projectile tumbling behavior because the

cavity shadow obliterated projectile attitude information. Lundstrom[14] has shown that if detailed projectile tumbling behavior is included the pulse shape during the drag phase can be matched with experimental results. The present results show that peak drag phase pressures may be estimated accurately using only an estimate of the average drag coefficient of the projectile as it traverses the tank.

Patterson[12] has measured the internal pressures for the same tank but with an .05 inch thick aluminum entry wall. Figures II-8 and 9 show a comparison of the Lundstrom prediction (assuming the entry wall is a free surface) and these experiments. Figure III-10 shows that the peak pressure versus radius is again accurately predicted by the Lundstrom analysis.

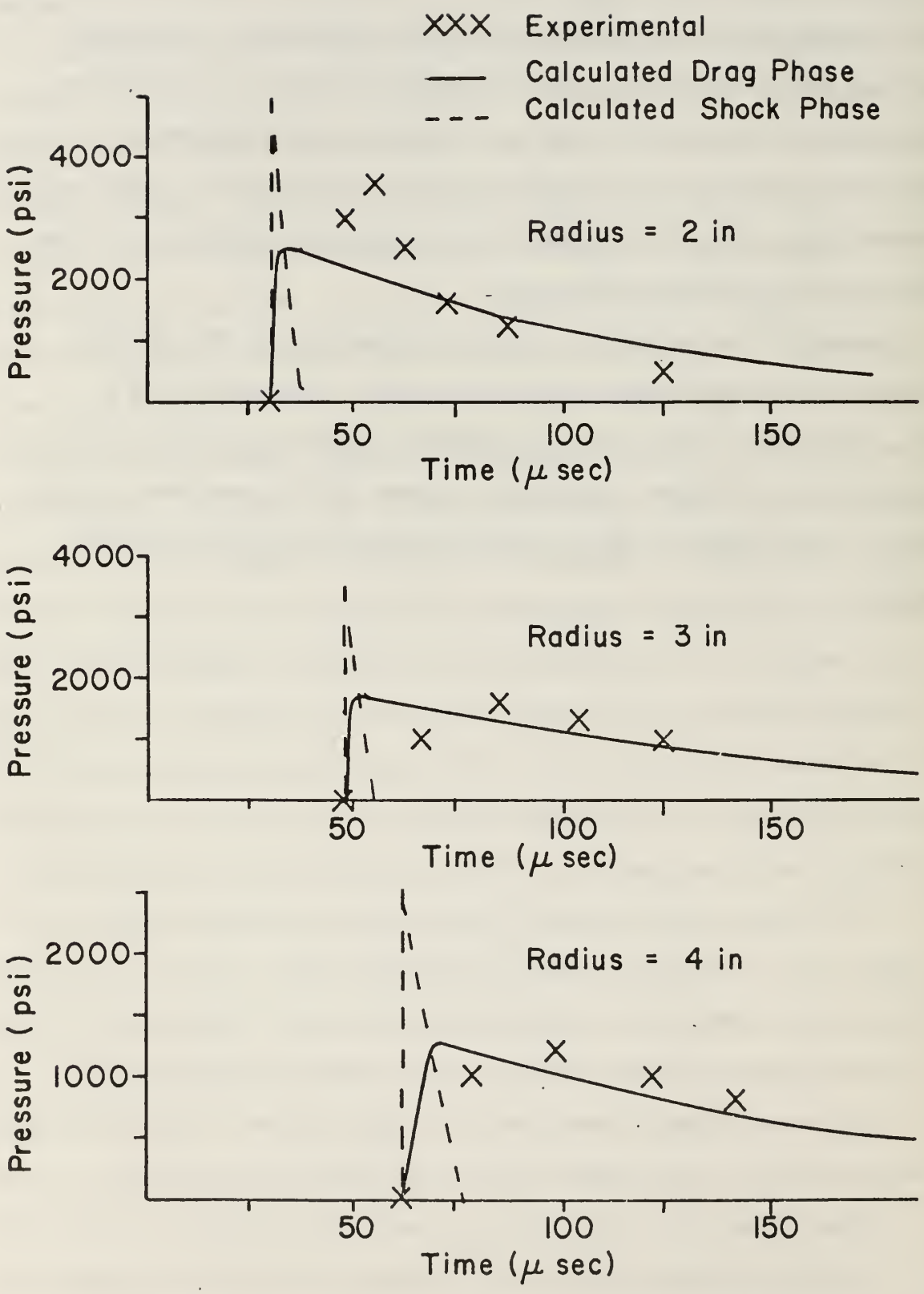

FIGURE III-1 PRESSURE COMPARISON
E_o = 7,493 IN.LB., HEAVY WALL

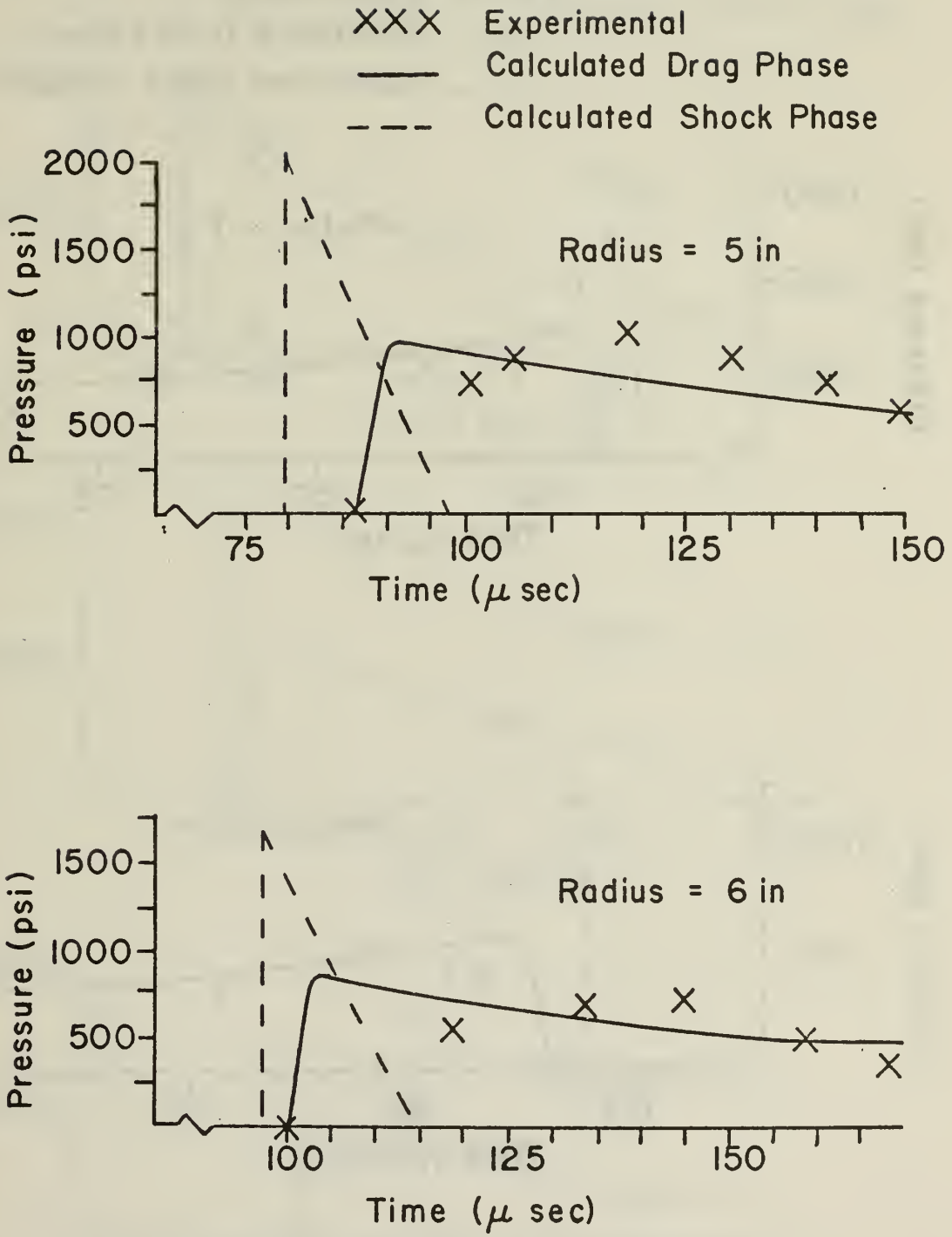

FIGURE III-2 PRESSURE COMPARISON
E_o = 7,493 IN. LB., HEAVY WALL

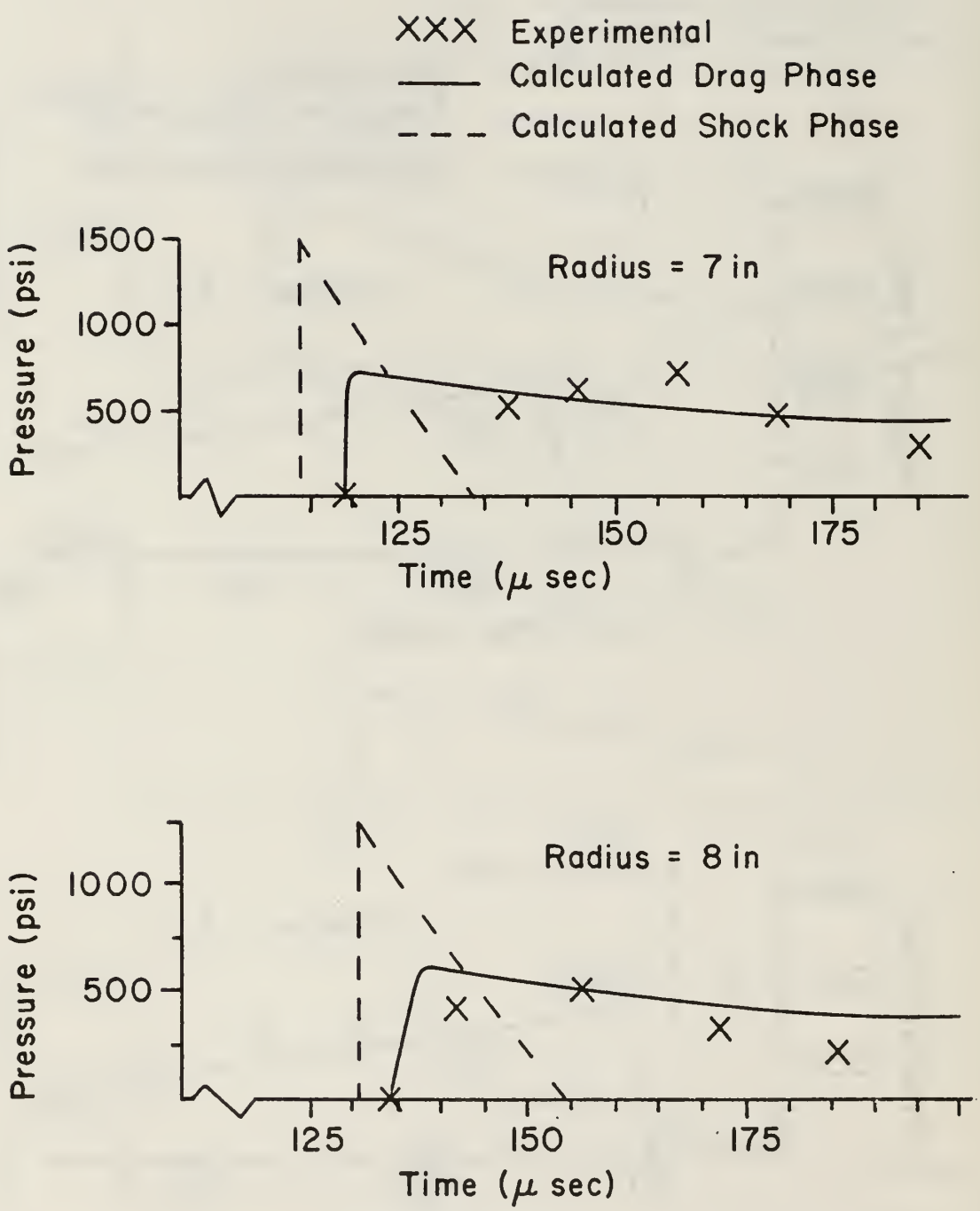

FIGURE III-3 PRESSURE COMPARISON
E_0 = 7,493 IN. LB., HEAVY WALL

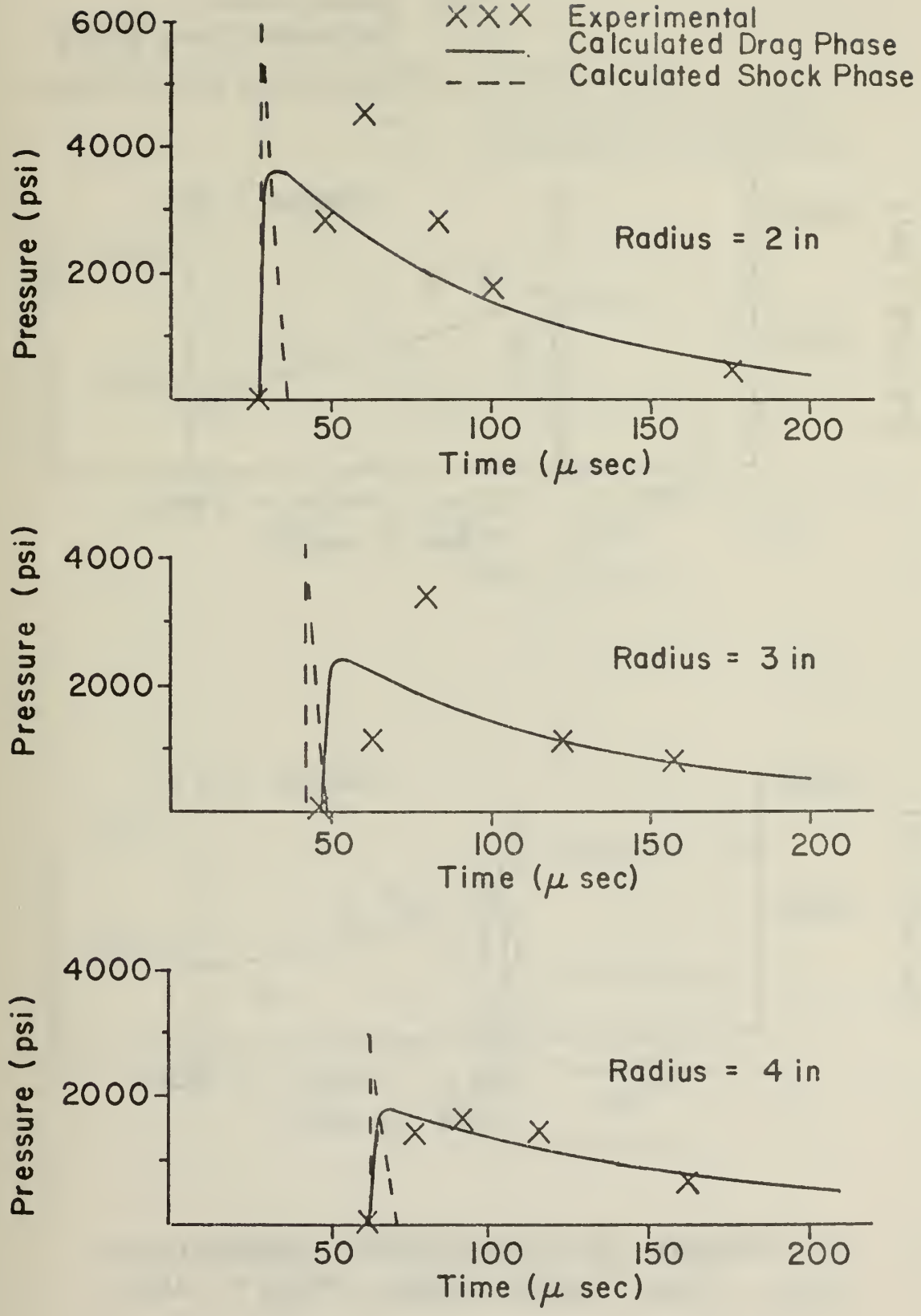

FIGURE III-4 PRESSURE COMPARISON
E_o = 12,323 IN. LB., HEAVY WALL

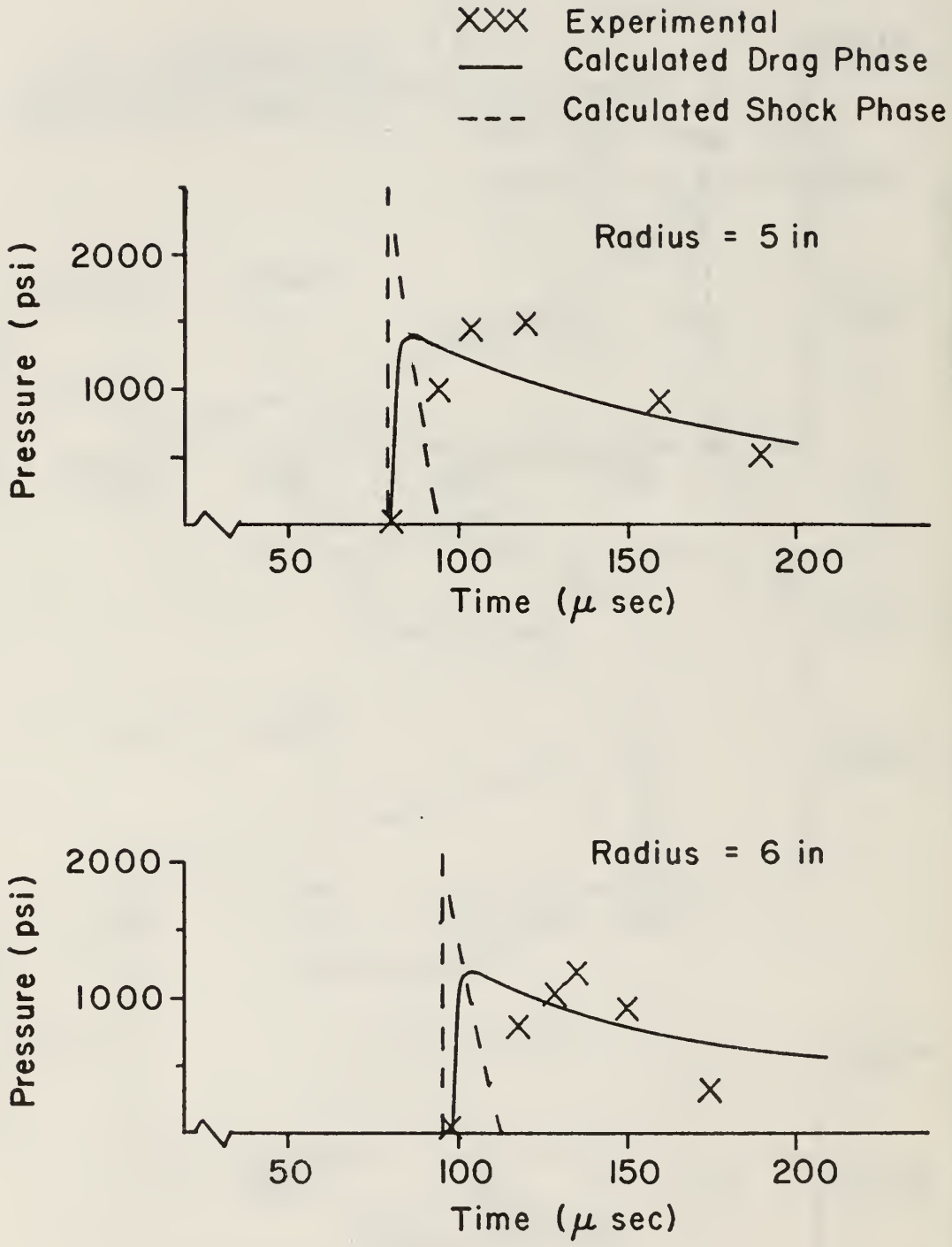

FIGURE III-5 PRESSURE COMPARISON
E_o = 12,323 IN. LB., HEAVY WALL

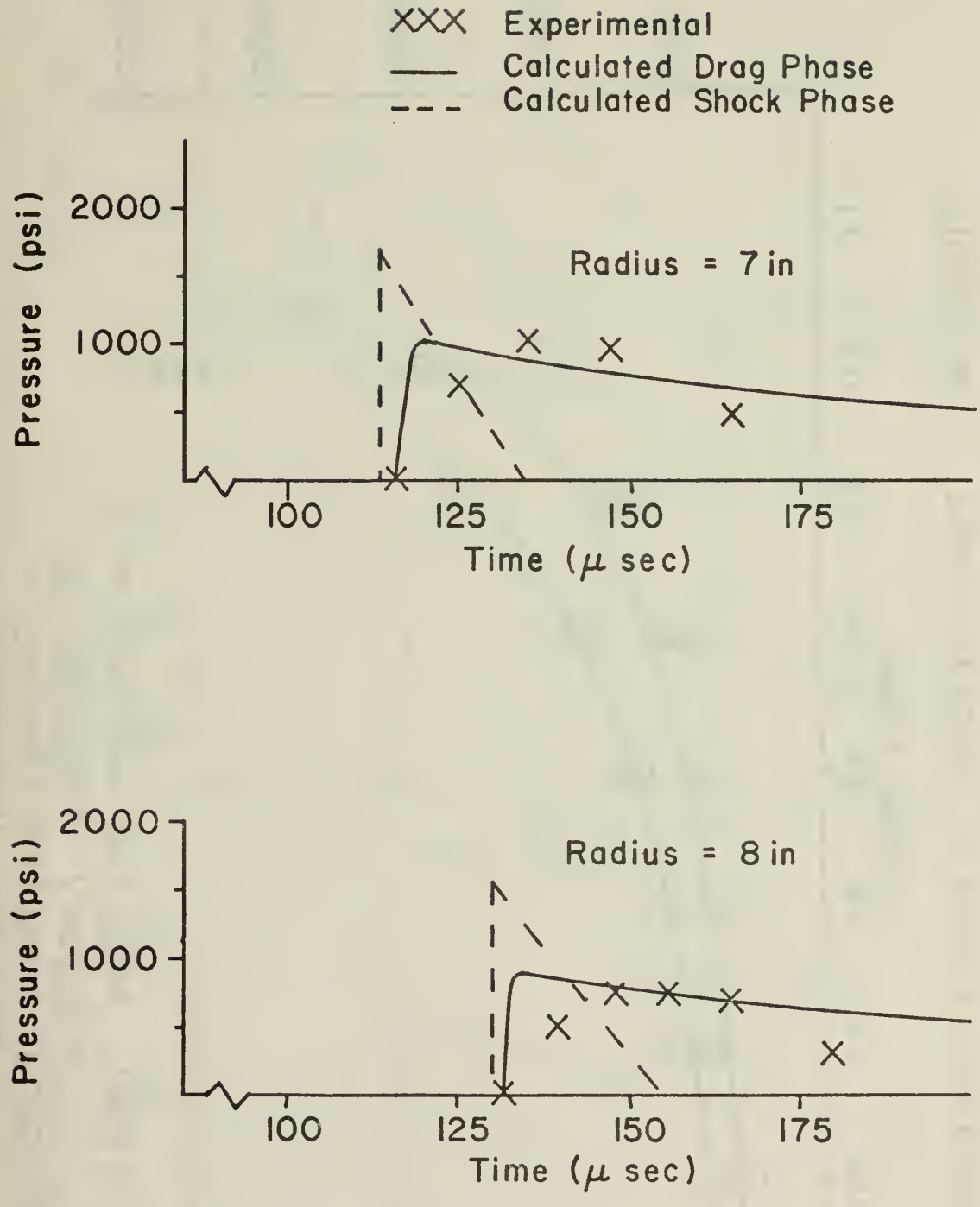

FIGURE III-6 PRESSURE COMPARISON
E_o = 12,323 IN.LB., HEAVY WALL

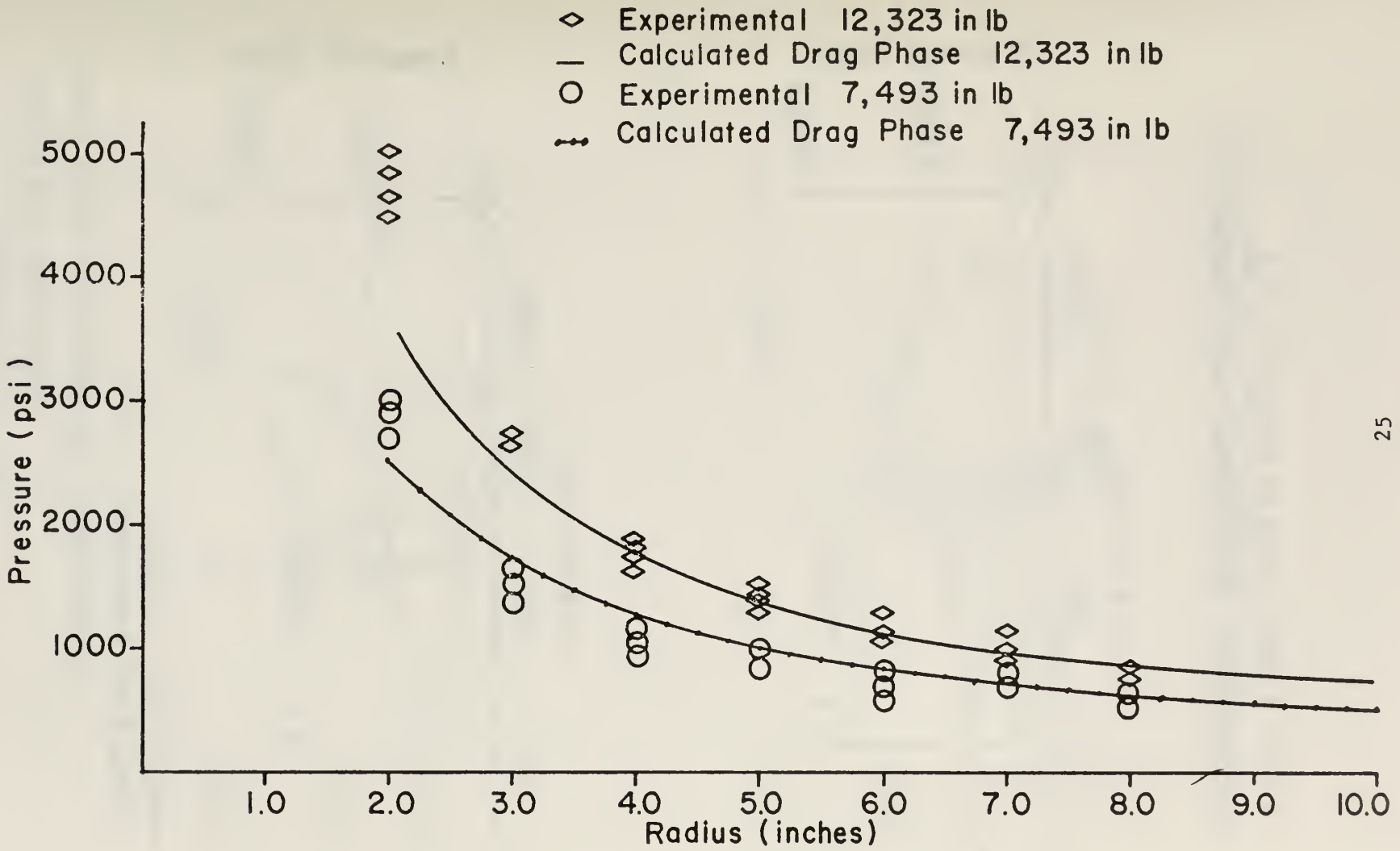

FIGURE III-7 PEAK PRESSURE vs. RADIUS FOR HEAVY WALL

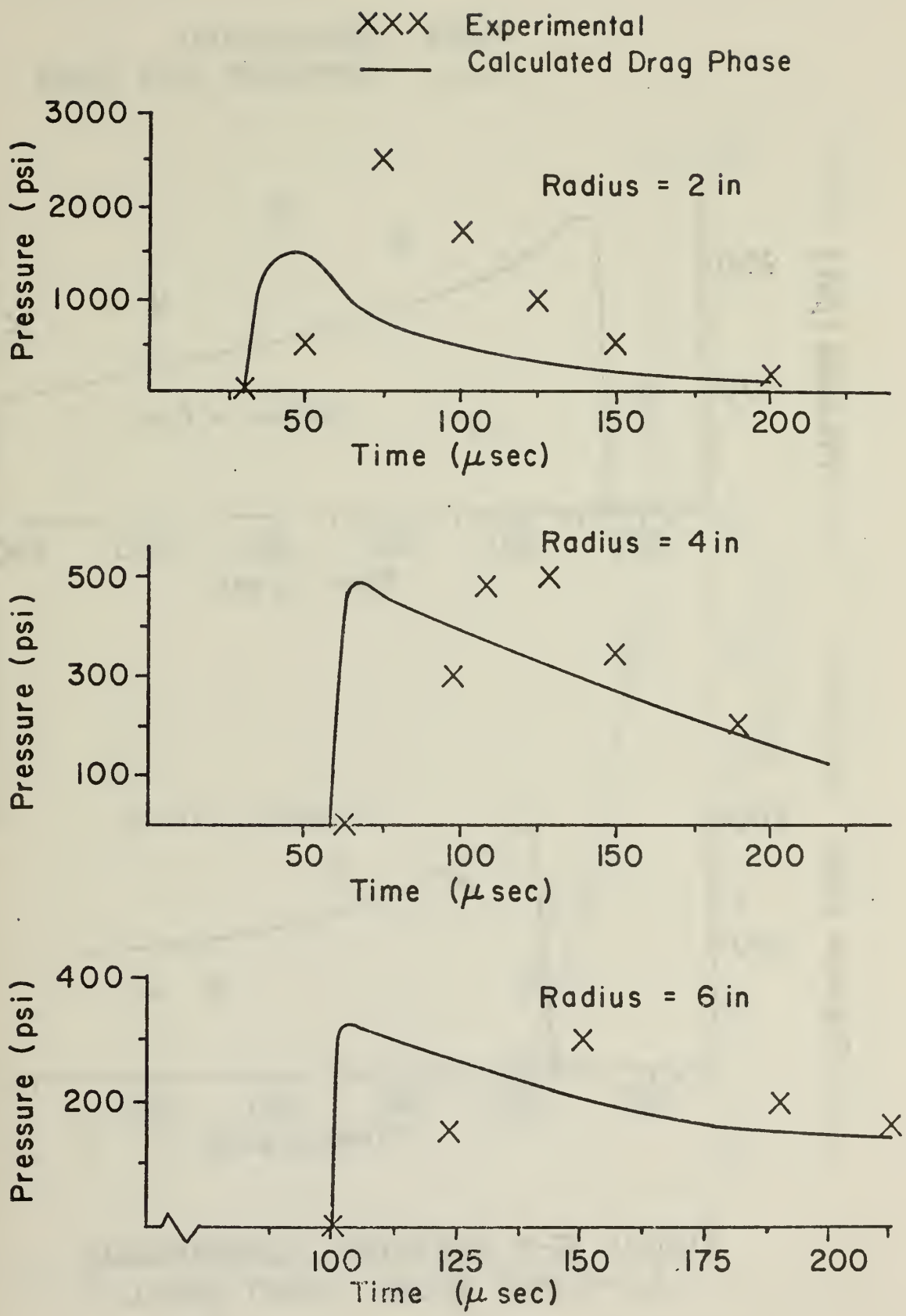

FIGURE III-8 PRESSURE COMPARISON
E_0 = 7,493 IN. LB., LIGHT WALL

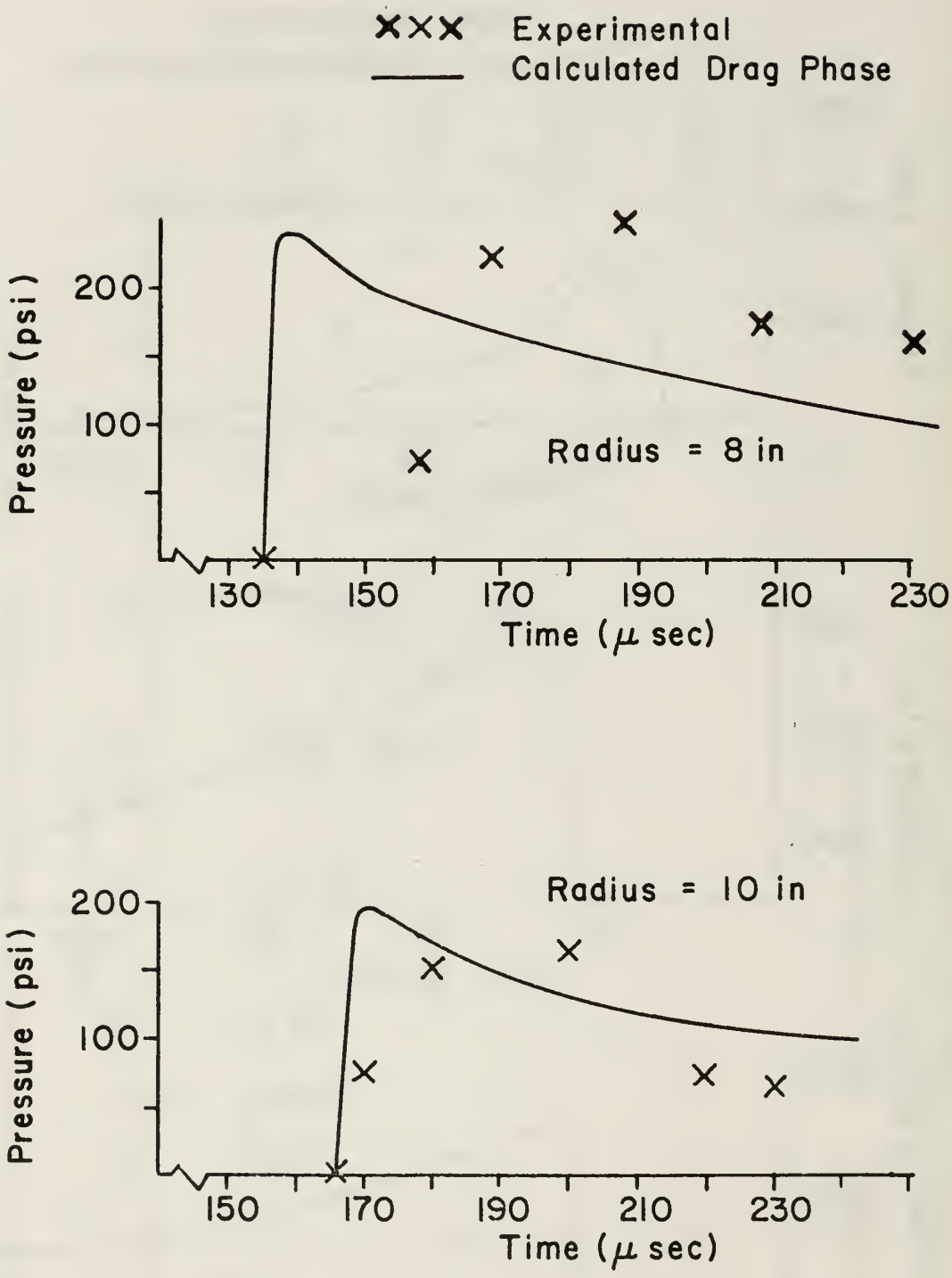

FIGURE III-9 PRESSURE COMPARISON
E_o = 7,493 IN.LB., LIGHT WALL

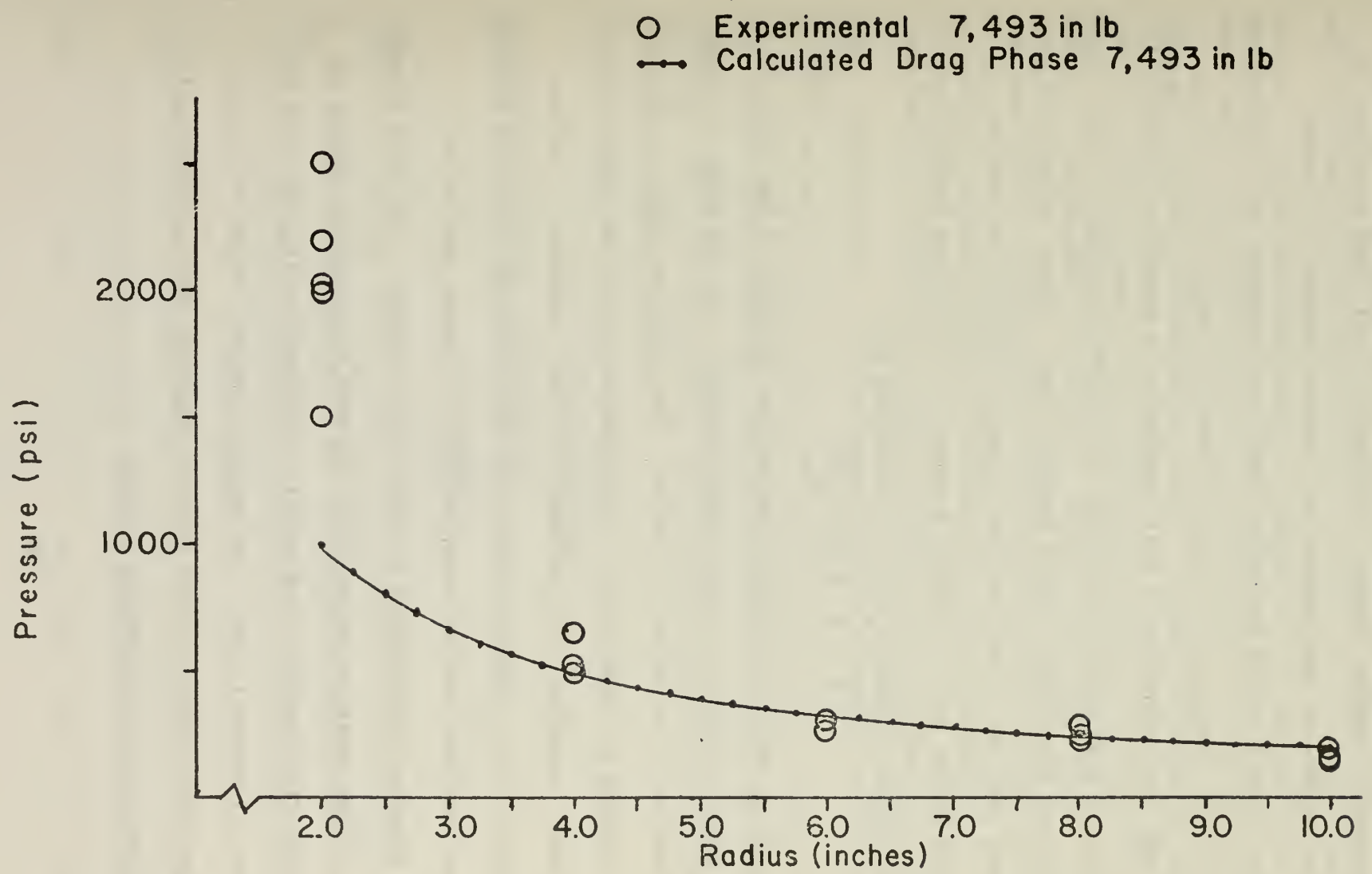

FIGURE III-10 PEAK PRESSURE vs. RADIUS FOR LIGHT WALL

IV. Fuel Cell Entry Wall Response During the Shock and Drag Phases

The estimation of fluid-filled tank wall response during hydraulic ram is extremely complex because the structural and fluid equations of motion are coupled by the presence of a common boundary. An exact prediction of wall strain and motion therefore, required the simultaneous solution of the structural and fluid differential equations of motion.

To make the prediction of wall response more tractable, Ball's[8,9,10] application of piston theory was used to provide an estimate of the fluid and structural interaction during hydraulic ram. Piston theory provides the correct solution to the one-dimensional propagation of stresses in an acoustic medium due to a moving boundary. This theory predicts that the wall pressure loading p_w may be calculated by:

$$p_w = p_i + \rho c\ (v_i - \dot{w}) \qquad \text{(IV-1)}$$

where p_i and v_i are the incident pressure and velocity of the fluid if the wall were not there, ρ is the fluid density, c is the speed of sound in the fluid and $\dot{w}$ is the wall velocity. The first two terms in the wall pressure loading are independant of wall motion, hence the application of piston theory uncouples the structural and fluid equations of motion. Wall response can be computed using only the structural equations modified to include the third term of equation IV-1 if a known prediction of incident pressure and velocity is used as the loading. The fluid dynamic analyses of the previous two sections was used to provide estimates of the incident fluid pressure and velocity generated during the shock and drag phases of hydraulic ram. The computer program SATANS was modified to include piston theory and was used to calculate the resulting wall response due to the time varying loading.

Experimental Results

A series of experiments[16] were undertaken to determine the entry wall response to shock and drag phase loadings for two threat energy levels. 7075-T6 Aluminum plates of thickness 0.05, 0.09 and 0.16 inches were tested. Each entry wall had four EA-13 type 175 ohm strain gages mounted 2 inches from the impact point. One pair of gages was oriented radially with one gage on the inside and the other on the outside of the plate. A second pair of gages was oriented circumferentially. The simple constant current strain gage circuit shown in Figure IV-1 was used to measure the dynamic response. The recording system consisted of a dual-beam oscilloscope with two 1A7 pre-amp plug-in units with differential input capability and a Polaroid scope camera. The effects of hydrostatic pressure on the wet gage output was neglected because it was found to be only 2 to 5 micro-inches per inch of indicated compressive strain per 1000 psi. The constant current circuit used in this experiment has a calibration equation given by

$$\frac{e}{\epsilon} = IR_g K \frac{\eta}{1-(1-\eta)\,\epsilon K} \qquad \text{(IV-1)}$$

where the efficiency η is given by:

$$\eta = \frac{R_2}{R_2+R_g} \qquad \text{(IV-2)}$$

where K is the gage factor, I the current, R_2 the load resistance, and R_g the active gage resistance. For the circuit elements shown in Figure IV-1 the calibration equation was simplified to the linear relationship:

$$\epsilon = 0.3529e \qquad \text{(IV-3)}$$

which was used to calculate surface strain from the measured voltage output.

Two .222 caliber projectile energy levels were tested for each of the three test plates. Shots taken at the higher energy level resulted

in considerable tank leakage and strain gage failure. High energy shots with the 0.05 inch thick plate resulted in permanent plate deformation that was not evident at the lower energy level. Significant deterioration of the strain gage bond accompanied each shot at the high energy level. As a result, less data are available at that energy level.

Figure IV-2 shows typical experimental entry wall strain measurements versus time for a 0.09 inch thick wall when impacted by the 7493 in-lb energy projectile. Additional data and analysis are contained in reference 16. The upper photograph shows that the radial strain is due to pure bending for approximately 60 μ seconds after impact. After this time some radial stretching is evident but both traces return to neutral at approximately 200 μ seconds. The dry (outside gage) continues below the neutral reading because of stretching but the relatively symmetrical variations from that point on show the continuation of back and forth bending. The lower photograph shows that circumferential strains are also primarily due to pure bending of the plate for the first 60 μ seconds. The circumferential strains, however, do not return to neutral which is indicative of stretching. The maximum strain amplitude of both radial and circumferential traces was approximately 1.4×10^{-3} in/in.

In order to evaluate the adequacy of piston theory for predicting the entry wall structural response, three different cases were calculated using SATANS. Each case used an incident shock phase pressure loading that was calculated using the computer program discussed in section II and a drag phase pressures loading predicted by the computer program of Lundstrom discussed in section III.

The first case assumed no fluid-wall interaction. The wall loading was taken to be the incident pressure p_i and $pc(v_i-\dot{w})$ terms of piston

theory were neglected. Figures IV-3 and 4 show a comparison of this result with the experiment. Predicted wall strains are very large compared with those measure experimentally because the reduction of fluid pressure at the wall due to wall motion has been ignored. The strain predictions indicate that the entry wall should sustain a permanent set. Experimental entry walls show no such behavior. It is clear that the inclusion of the fluid-wall interaction is necessary of reasonable wall response predictions are to be made during hydraulic ram.

The second entry wall response assumed that the fluid-wall interaction could be modeled by piston theory. The wall loading was calculated by $p_i + \rho c v_i$ where the velocity v_i was taken as the normal component of the incident fluid velocity at the wall. SATANS was modified by Ball to include the $\rho c \dot{w}$ term in the structural equation of motion. The results of these calculations are shown in Figures IV-5 and 6. These figures show that the predicted strains are considerably larger than measured. Figures 7 through 9 show the assumed loadings of the plate (p_i and $p_i + \rho c v_i$) at three times during the response calculation. The net pressure at the entry wall ($p_i + \rho c(v_i - \dot{w})$) is also plotted in these figures. An examination of these figures shows a very large loading of the plate center due to the $\rho c v_i$ term. This large loading of the plate center is responsible for the overestimation of wall strains. The one-dimensional $\rho c v_i$ term is clearly not a good estimate of reflected wave momentum near the plate center where the flow is very three-dimensional.

The third wall response prediction assumed that the wall loading could be given by $2p_i$. This loading corresponds to assuming that the $\rho c v_i$ term can be replaced by p_i as in the case of waves reflecting off a rigid wall. Figures IV-10 and 11 compare this modified piston theory

prediction and the experimental results. Figures IV-7 through 9 show that the large loading at the center of the plate has been eliminated. As a result the predicted strains are much closer to those measured. Figures 7 through 9 also show that the modified piston theory net wall pressure ($2p_i - \rho c\dot{w}$) is negative toward the center of the plate. This indicates that the wall has moved too quickly out of the way in response to the fluid pressure loading. The resulting negative wall pressure is responsible for the descrepancy between measured and predicted strains. The negative net pressure may be eliminated by limiting the wall velocity to values for which the net pressure is zero.

Figures IV-10 and 11 show a peak strain at 35 μ seconds which corresponds to the arrival of the shock front at the gage location. The predicted strains decrease only to increase again as the effects of the drag phase pulse are felt. The experimental results do not exhibit the characteristics of the first calculated peak which indicates that the wall does not respond to the shock phase as predicted. The prediction underestimates the wall strain due to the drag phase because of the existance of negative net pressure at the wall. The agreement of theory and experiment is, however, much better than any previous theory has obtained. It is concluded, therefore, that the modified piston theory can be used to give reasonable estimates of fuel cell wall response during hydraulic ram.

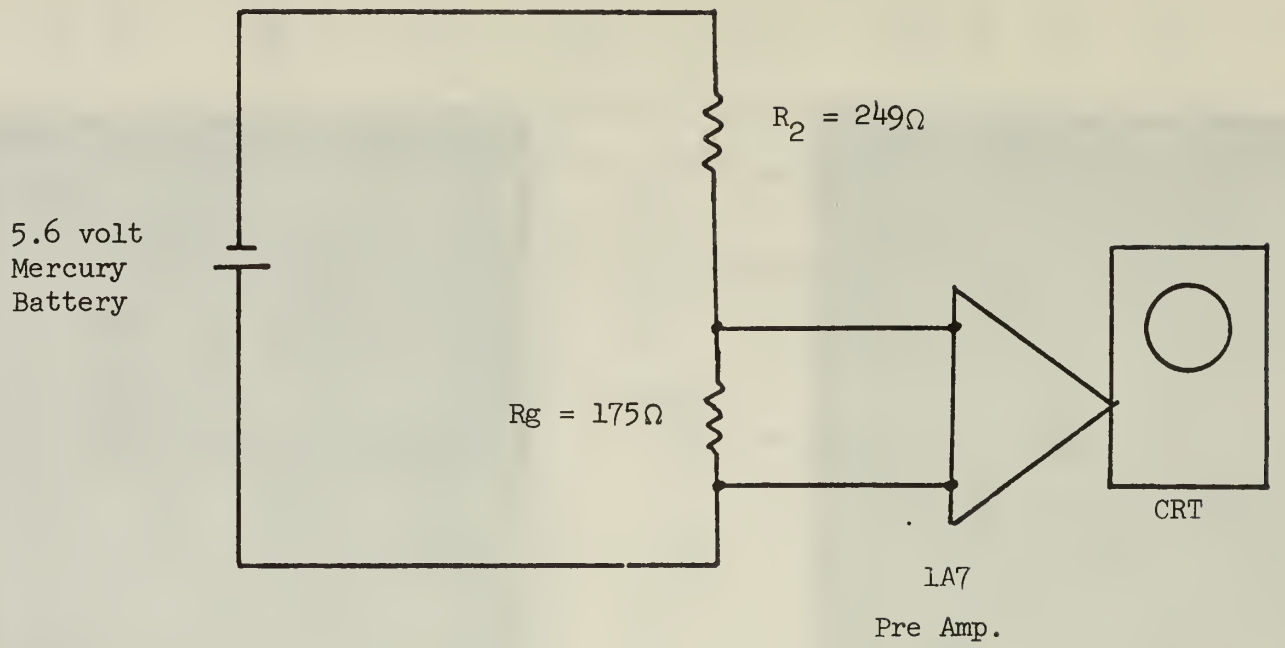

Figure IV-1 Dynamic Strain Gage Circuit

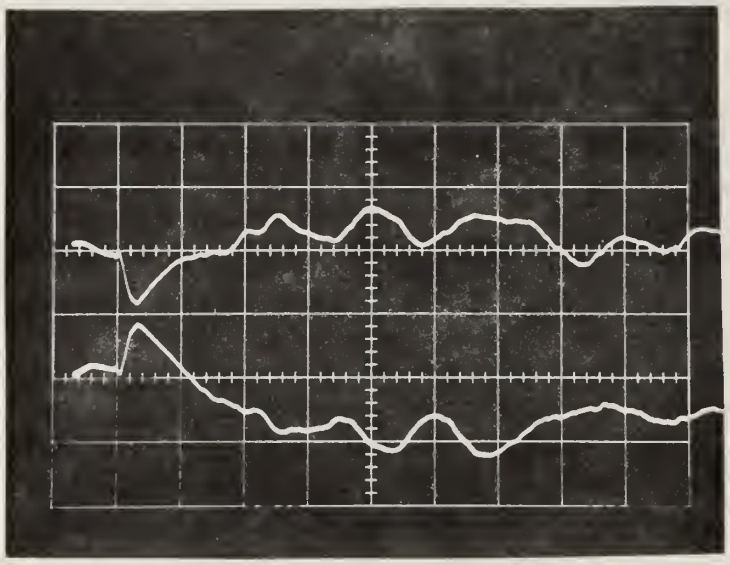

Radial Gages

200μsec/cm 5 mvolts/cm

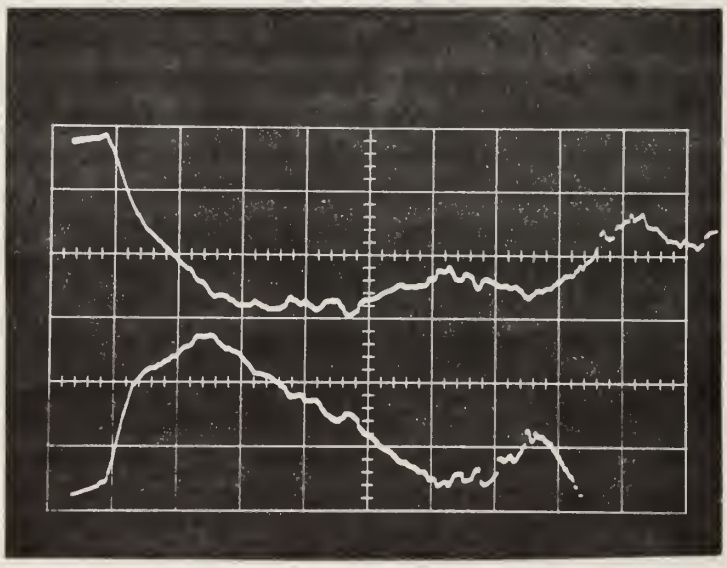

Circumferential Gages

200μsec/cm 2 mvolts/cm
h (thickness) = .09 in.

Figure IV-2. Entry Wall Strain (E_o= 7493 in-lb)

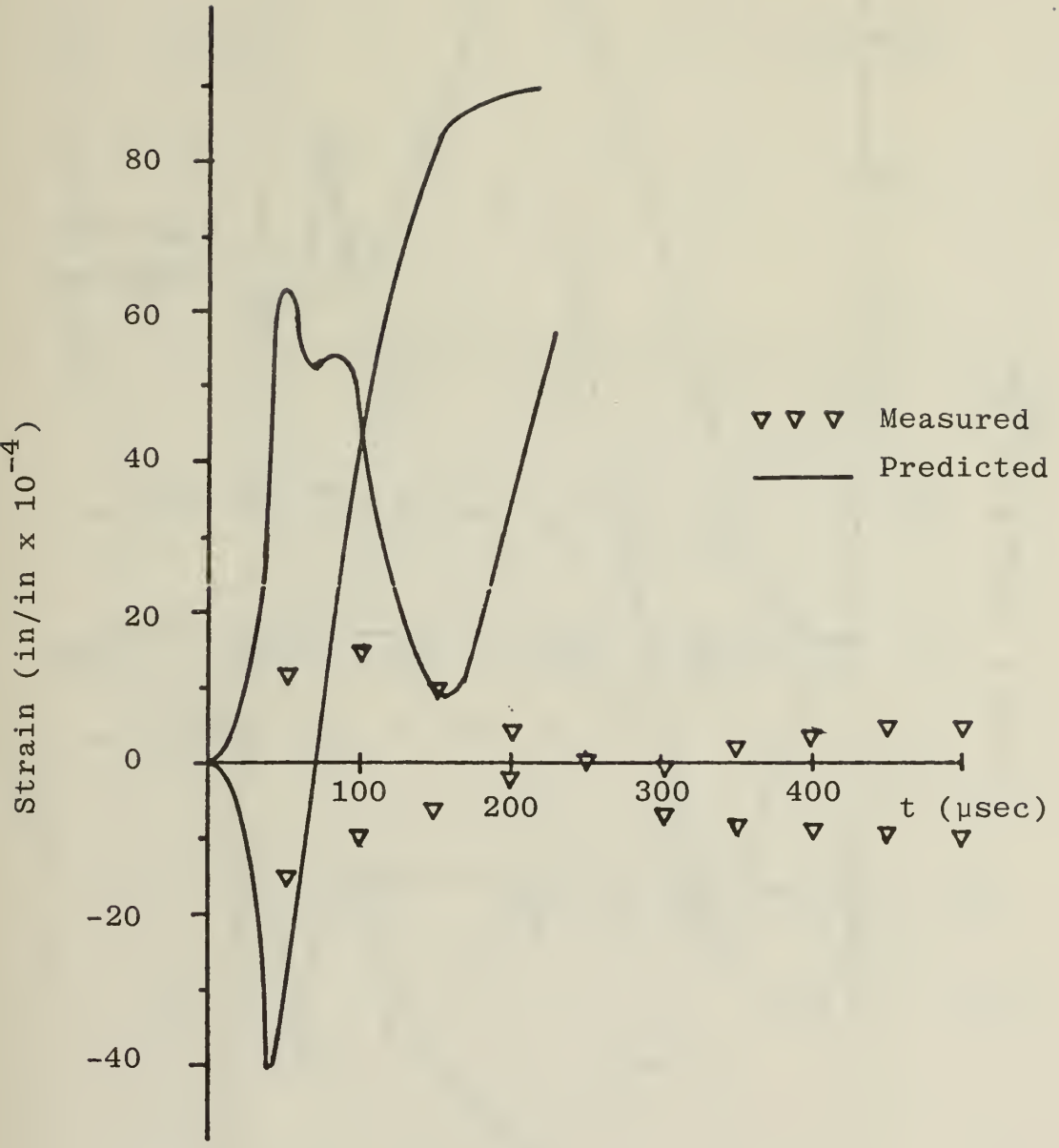

Figure IV-3 Radial Wall Strain Without Fluid-Wall Interaction

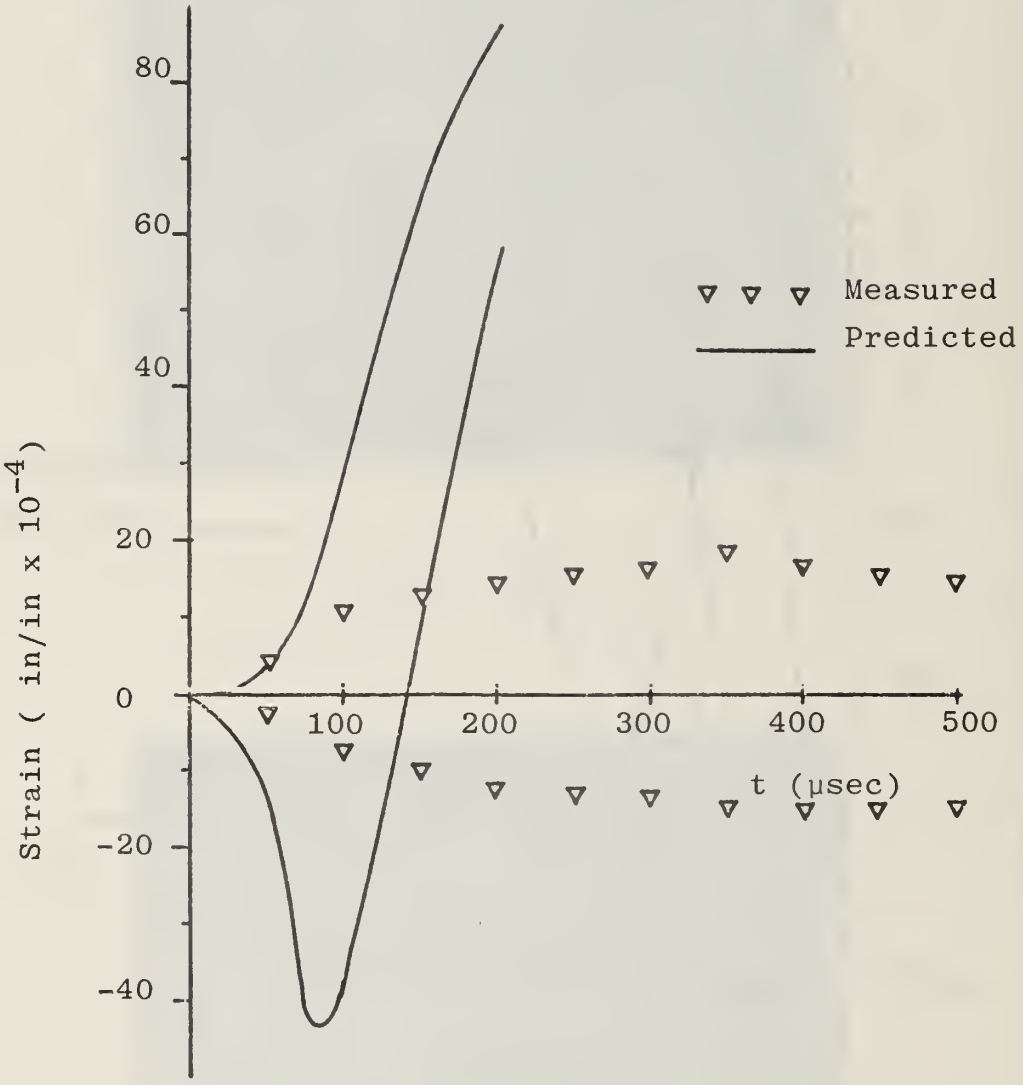

Figure IV-4. Circumferential Wall Strain Without Fluid-Wall Interaction

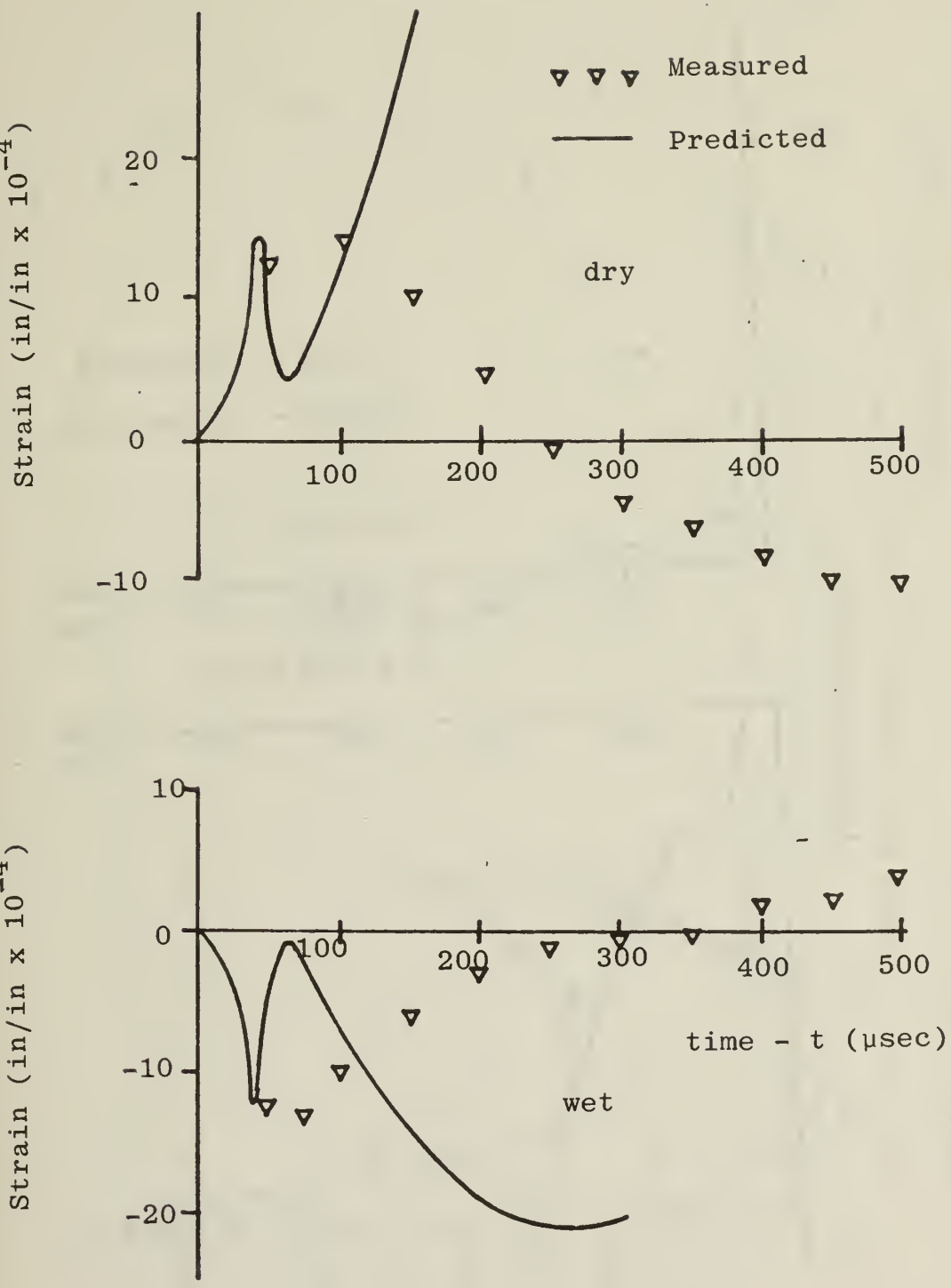

Figure IV-5. Radial Wall Strain With Piston Theory

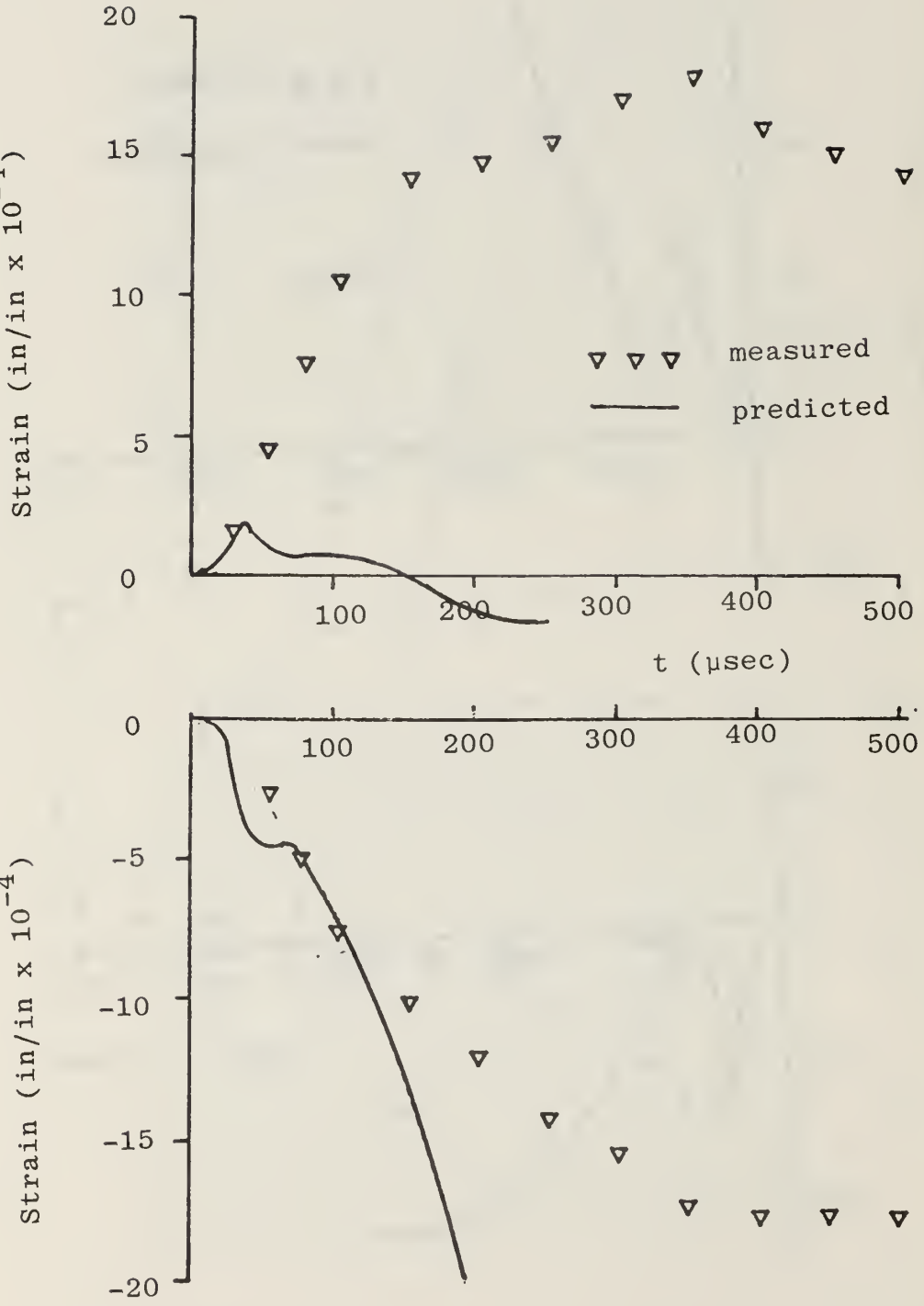

Figure IV-6. Circumferential Wall Strain With Piston Theory

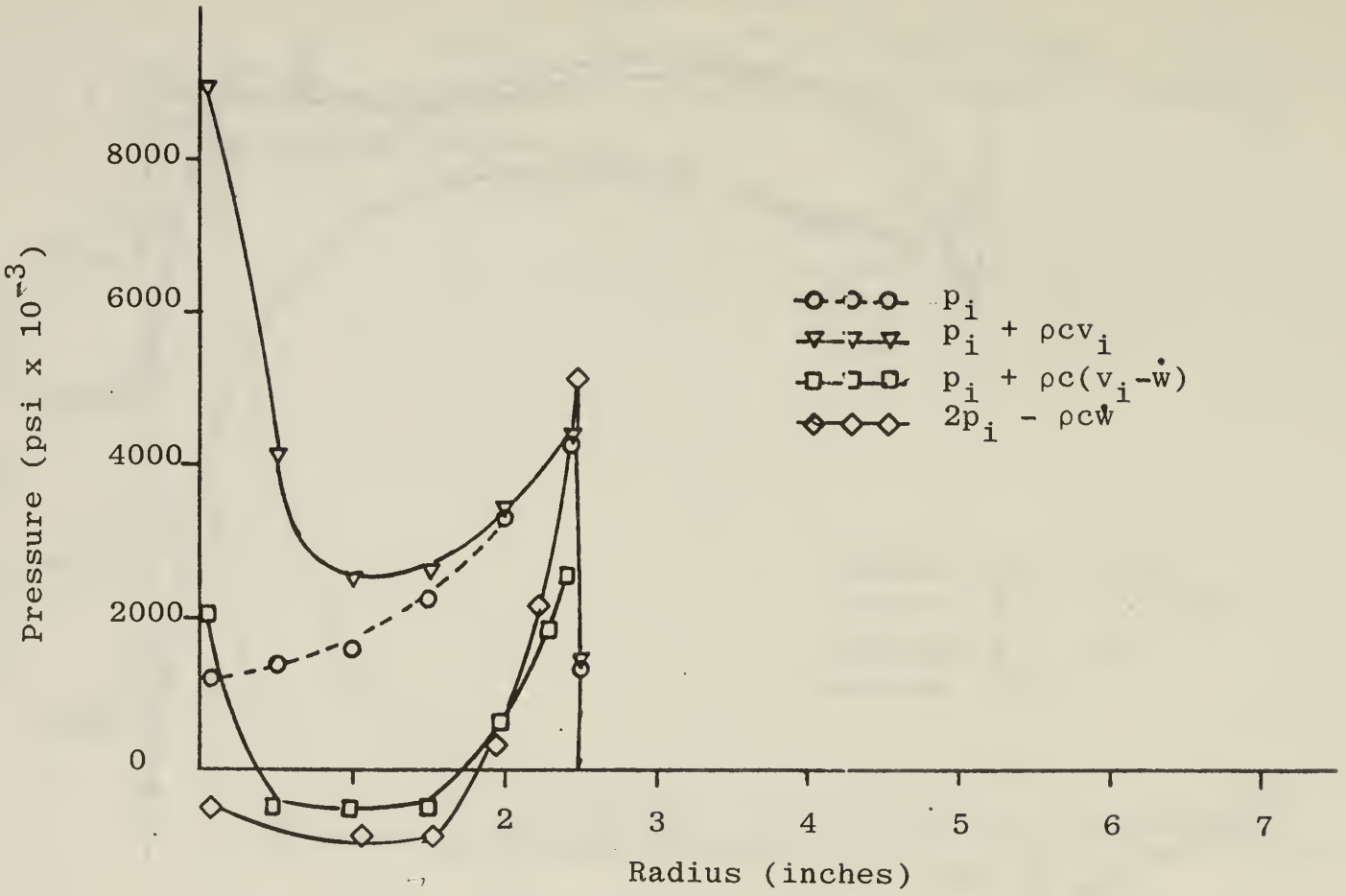

Figure IV-7. Entry Wall Pressure 50 μsec After Impact

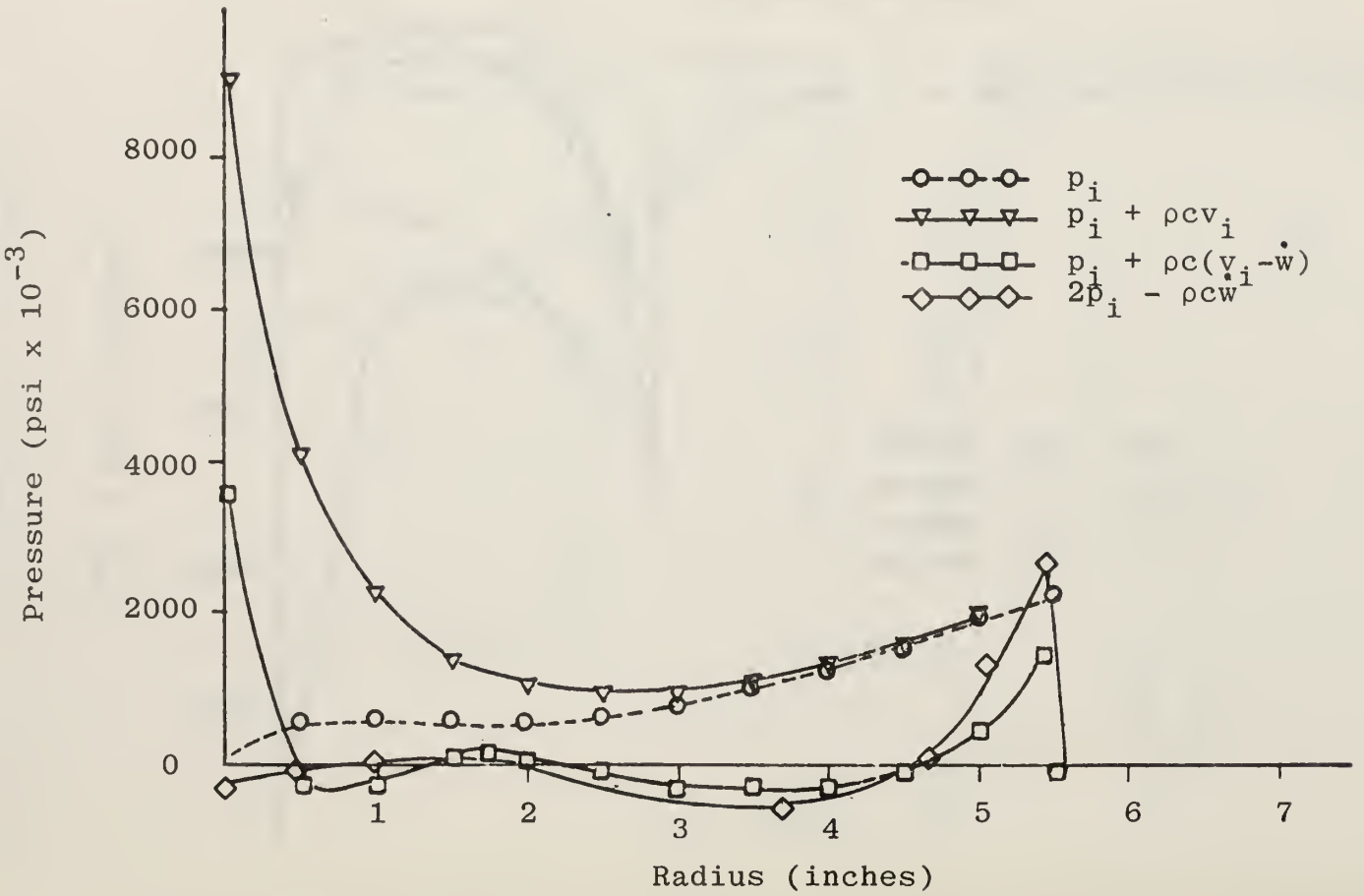

Figure IV-8. Entry Wall Pressure 100 μsec After Impact

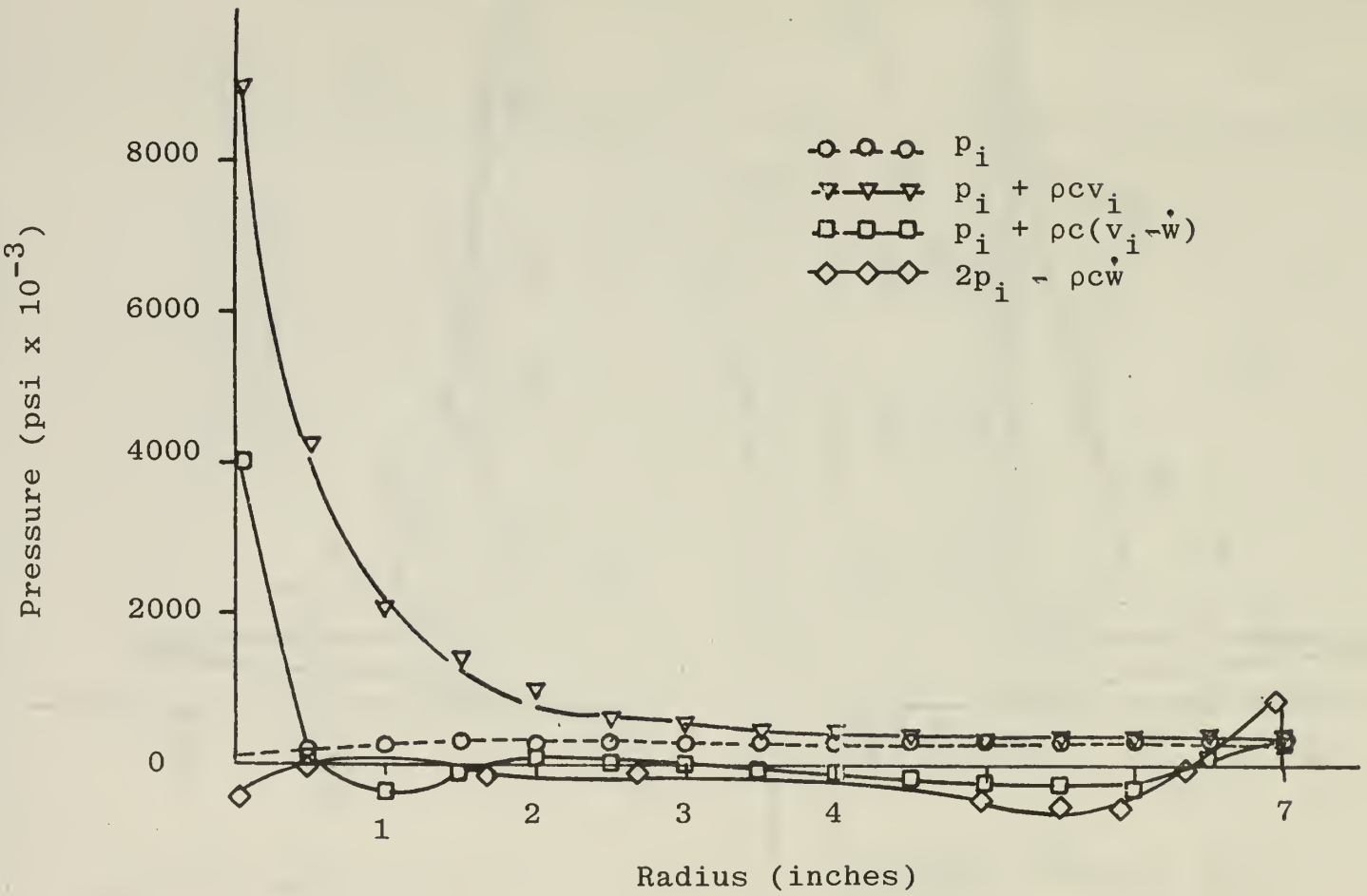

Figure IV-9. Entry Wall Pressure 150 μsec After Impact

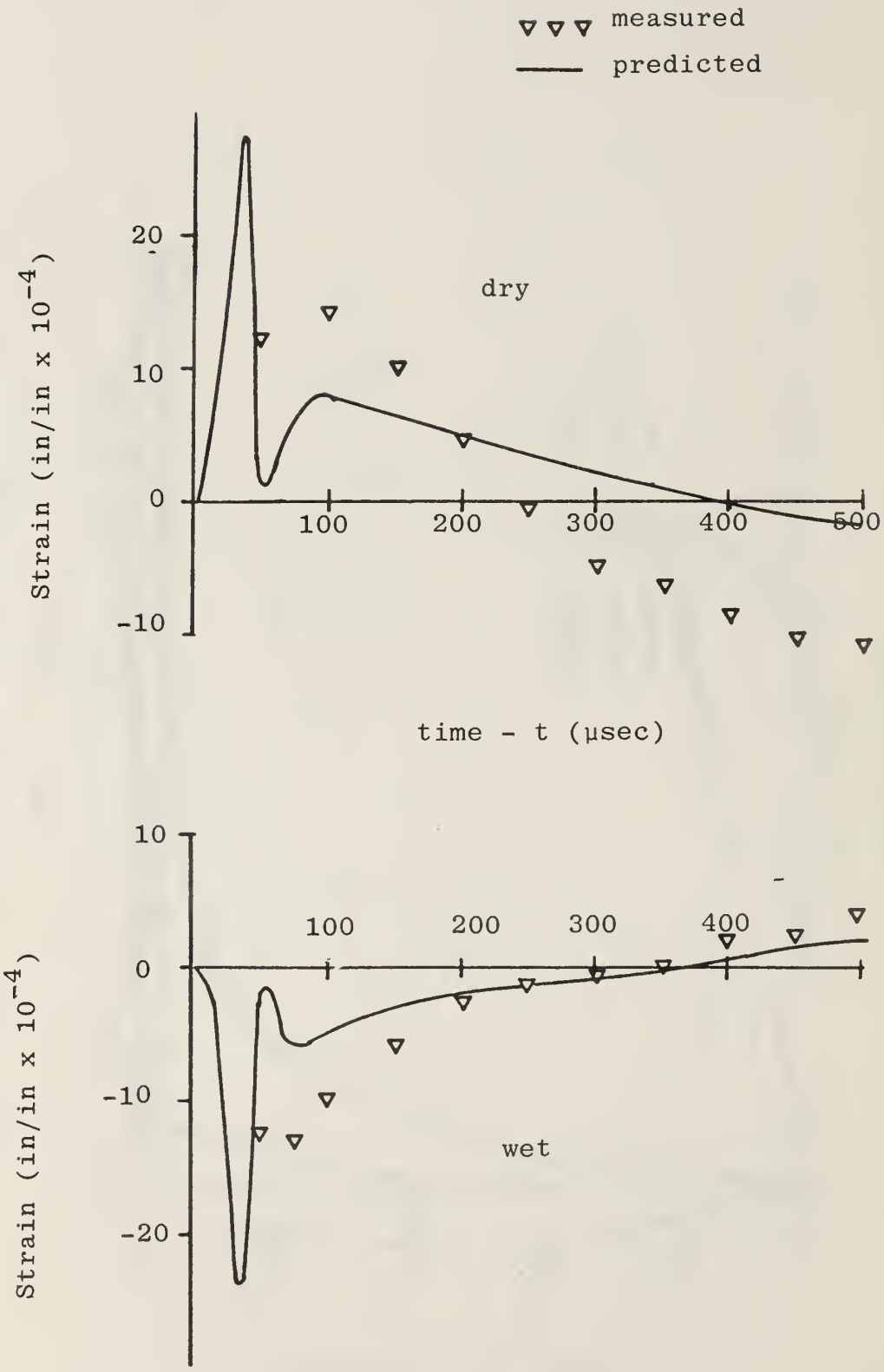

Figure IV-10. Radial Wall Strain With Modified Piston Theory

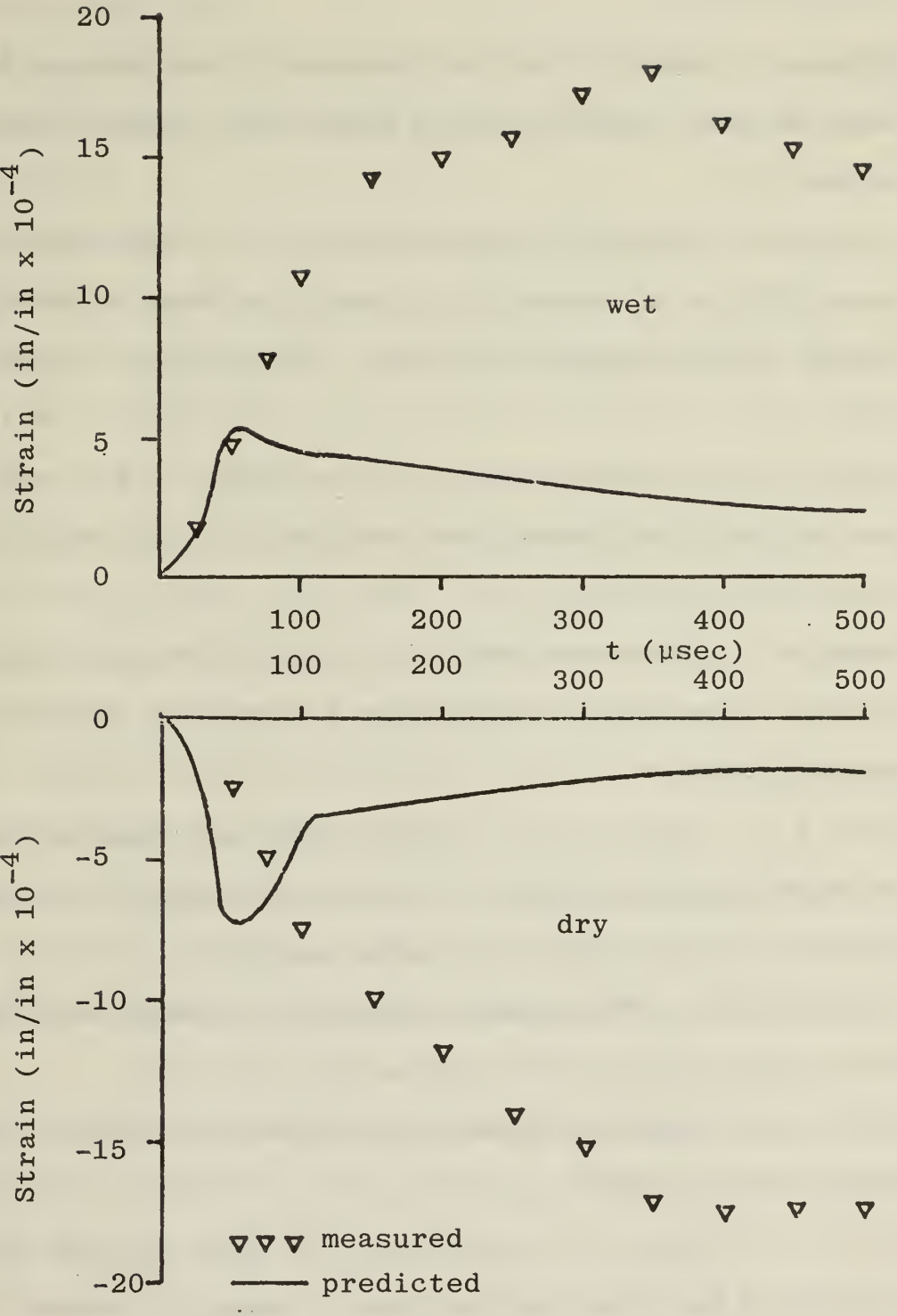

Figure IV-11. Circumferential Wall Strain with Modified Piston Theory

V. References Cited

1. McMillen, J. Howard, "Shock Wave Pressures in Water Produced by Impact of Small Spheres," Physical Review, Vol. 68, Nos. 9 and 10, November 1945.

2. Stepka, F. S., Morse, R. C., and Dengler, R. P., "Investigation of Characteristics of Pressure Waves Generated in Water Filled Tanks Impacted by High-Velocity Projectiles, " NASA TN D3143, December 1965.

3. Kapple, L. S., "Hydraulic Ram Shock Phase Effects on Fuel Cell Survivability," MSAE Thesis, Naval Postgraduate School, Monterey, California, March 1974.

4. Yurkovich, R., "Hydraulic Ram: A Fuel Tank Vulnerability Study," McDonnell Aircraft Engineering Methods Authorization, F65-76-555, September, 1969.

5. Power, H. L., "Fluid Dynamic Analysis of The Shock Phase of Hydraulic Ram (User's Manual for Pressure Model)", NPS-57Ph75062, Naval Postgraduate School, Monterey, California, June 1975.

6. Lundstrom, E. A., "Fluid Dynamic Analysis of Hydraulic Ram," Naval Weapons Center Technical Publication 5227, July 1971.

7. Cole, R. H., "Underwater Explosions," Princeton, New Jersey, Princeton University Press, 1948.

8. Ball, R. E., Power, H. L., and Fuhs, A. E., "Fuel Tank Wall Response to Hydraulic Ram During the Shock Phase," Journal of Aircraft, Vol. 10, No. 9, pp. 571-572, September, 1973.

9. Ball, R. E., "Aircraft Fuel Tank Vulnerability to Hydraulic Ram: Modification of the Northrup Finite Element Computer Code BR-1 to Include Fluid-Structure Interaction - Theory and Users Manual for

BR-1HR," NPS-57BP74071, Naval Postgraduate School, Monterey California, July 1974.

10. Fuhs, A. E., Ball, R. E., and Power, H. L., "FY73 Hydraulic Ram Studies," NPS-57Fu74021, Naval Postgraduate School, Monterey, California, February 1974.

11. Holm, C. M., "Hydraulic Ram Pressure Measurements," MSAE Thesis, Naval Postgraduate School, Monterey, California, December 1974.

12. Patterson, J. W., "Fuel Cell Pressure During Hydraulic Ram" MSAE Thesis, Naval Postgraduate School, Monterey, California, June 1975.

13 Winchester, H. F., Denlinger, J. F., Vickers, G. A., Dunbar, W. R., and Christensen, L. D., "Fuel Tank Vulnerability Reduction," MDC-J-0044, Douglas Aircraft Company, Long Beach, California, April 1970.

14. Lundstrom, E. A., and Fung, W. K., "Fluid Dynamic Analysis of Hydraulic Ram III (Result of Analysis)," Joint Technical Coordinating Group Aircraft Survivability Report TEAS P.E. 5.1.1.11, Naval Weapons Center, China Lake, California, October 1974.

15. Ball, R. E., "A Computer Program for the Geometrically Nonlinears Static and Dynamic Analysis of Arbitrarilly Loaded Shells of Revolution, Theory and Users Manual" NASA Contractor Report NASA CR-1987, April 1972.

16. Page, B. D., "Fuel Cell Entry Wall Response to Hydraulic Ram", MSAE Thesis, Naval Postgraduate School, Monterey, California, March 1975.

VI. List of Figures

DISTRIBUTION LIST

		No. of Copies
1.	Library Code 0212 Naval Postgraduate School Monterey, CA 93940	2
2.	Department of Aeronautics Code 57 Naval Postgraduate School Monterey, CA 93940	
	Prof. R. W. Bell, Chairman	1
	Prof. H. L. Power	2
	Prof. R. E. Ball	6
3.	Defense Documentation Center Cameron Station Alexandria, VA 22314	12
4.	Mr. Wallace K. Fung Code 5114 Naval Weapons Center China Lake, CA 93555	20
5.	Dean of Research Naval Postgraduate School Monterey, CA 93940	1